European Journal of Medicinal Chemistry 46 (2011) 5959–5969

Contents lists available at SciVerse ScienceDirect

European Journal of Medicinal Chemistry

journal homepage: http://www.elsevier.com/locate/ejmech

Original article

Sugar-based peptidomimetics inhibit amyloid β-peptide aggregation

Bertrand Dorgeret [a,1], Lucie Khemtémourian [b,1], Isabelle Correia [b], Jean-Louis Soulier [a], Olivier Lequin [b,**], Sandrine Ongeri [a,*]

[a] Molécules Fluorées et Chimie Médicinale, BioCIS UMR-CNRS 8076, IPSIT, LabEx LERMIT, Université Paris-Sud 11, Faculté de Pharmacie, 5 rue Jean-Baptiste Clément, 92296 Châtenay-Malabry Cedex, France
[b] UPMC Univ Paris 06, Laboratoire des Biomolécules, UMR 7203 CNRS-UPMC-ENS, 4 place Jussieu, 75252 Paris Cedex 05, France

ARTICLE INFO

Article history:
Received 28 July 2011
Received in revised form
30 September 2011
Accepted 4 October 2011
Available online 12 October 2011

Keywords:
Amyloid β-peptide
Aggregation
Inhibitor
Peptidomimetics
IAPP

ABSTRACT

Alzheimer's disease is characterized by the oligomerization and amyloid fibril formation of amyloid β-peptide (Aβ). We describe a novel class of small water-soluble Aβ binding peptidomimetics based on two hydrophobic Ala-Val and Val-Leu dipeptides linked to a D-glucopyranosyl scaffold through aminoalkyl and carboxyethyl links in C1 and C6 positions. These compounds combine the targeting of hydrophobic recognition interfaces with an original hydrophilic sugar β-breakage strategy. These molecules were shown, by fluorescence thioflavin-T assays, to dramatically slow down the kinetics of amyloid fibril formation even at a low peptidomimetics to Aβ ratio of 0.1:1. Electron microscopy images revealed that the peptidomimetics efficiently reduced the amount of typical amyloid fibrils. NMR saturation transfer difference experiments indicated that these molecules interact with Aβ aggregated species through their hydrophobic amino acid residues. This inhibition effect was found to be sequence-specific since these molecules did not alter the kinetics of aggregation of another amyloid peptide, IAPP, involved in type 2 diabetes mellitus.

1. Introduction

Alzheimer's disease (AD) is one of the most common age-related neurodegenerative disorders, affecting more than 30 million people in the world, a number that is expected to double every 20 years [1]. AD is associated with the formation of extracellular amyloid fibrils by amyloid β-peptides (Aβ) and of intraneuronal paired helical filaments by the protein Tau [2]. The amyloid Aβ peptides, $A\beta_{1-40}$ and $A\beta_{1-42}$, are produced by the cleavage of the transmembrane amyloid β protein precursor [3]. In solution, the aggregation process of Aβ peptides involves a secondary structure transition from unordered/α-helix [4] to β-sheet conformation leading to cross β-sheet structure formation with β-strands perpendicular to the long fibril axis [5]. Distinct morphological species including oligomers, protofibrils, and fibrils are formed during the aggregation process [6]. Soluble oligomeric Aβ forms are thought to be mainly responsible for neurological toxicity [7–9]. However recent studies suggest that the toxicity of amyloid peptides is mediated by the fibrillation process rather than by discrete oligomeric species [10]. Therefore attractive strategies for treating AD aim at inhibiting the formation of amyloid fibrils and/or redirecting the aggregation cascade toward off-pathway species with reduced toxicity [11].

Several approaches have been used to inhibit the aggregation of soluble Aβ monomers, either by stabilizing native conformations [12] or by preventing β-strand intermolecular interactions using β-sheet binders [13]. The hydrophobic KLVFF sequence in the central region of Aβ peptide (residues 16–20) appears to be important for stabilizing intra- and intermolecular interactions involved in aggregation and amyloid formation [14]. Small peptides mimicking this hydrophobic sequence were demonstrated to modulate the kinetics of aggregation [13,15,16]. Furthermore, variants of this core domain incorporating β-sheet breaker amino acids such as *N*-methyl amino acids [17], proline [18] or α-amino-isobutyric acid [19] have proved to be valuable molecules for inhibiting Aβ peptide aggregation by destabilizing the pathological β-sheet conformation.

We describe herein a novel class of small water-soluble peptidomimetics based on flexible, sugar-based scaffolds, as inhibitors of Aβ aggregation (Fig. 1). These compounds incorporate two short hydrophobic dipeptide units, Ala-Val and Val-Leu that were chosen to interact with the hydrophobic regions of Aβ. These sequences are attached to a D-glucopyranosyl scaffold via an aminoalkyl and

* Corresponding author. Tel.: +33 146835737; fax: +33 146835740.
** Corresponding author. Tel.: +33 144273113; fax: +33 144277150.
E-mail addresses: olivier.lequin@upmc.fr (O. Lequin), sandrine.ongeri@u-psud.fr (S. Ongeri).
[1] These authors contributed equally to this work.

0223-5234/$ – see front matter © 2011 Elsevier Masson SAS. All rights reserved.
doi:10.1016/j.ejmech.2011.10.008

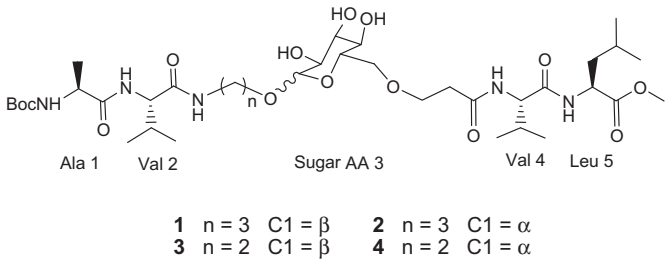

Fig. 1. Structure of peptidomimetics **1**–**4** containing D-glucopyranosyl sugar amino acid derivatives.

a carboxyethyl links in C1 and C6 positions, respectively (Sugar AA 3, Fig. 1). The carboxy and aminoalkyl linkers in our peptidomimetics were chosen to confer flexibility that may be necessary for optimal interaction of amino acid residues with the β-sheet Aβ target. The design of these peptidomimetics was inspired by previous strategies of Soto [18] and others [13–17] who described synthetic five residues β-sheet breaker pseudopeptides as inhibitors of Aβ aggregation. The originality of our peptidomimetics consists in the introduction of a central sugar moiety to perturb the regular interstrand hydrogen-bond network and destabilize β-sheet formation locally. We anticipated that these inhibitor peptidomimetics would operate mainly by binding to Aβ through their four hydrophobic amino acids at one hydrogen-bonding face and simultaneously hindering the interaction with other Aβ peptides thanks to the central sugar moiety acting as a β-sheet breaker element. The introduction of a carbohydrate in peptides can also have a multifaceted impact on the properties of peptides such as modulating the hydrophilicity/hydrophobicity balance, conferring peptide resistance to proteolytic cleavage [20], and promoting β-turn conformations [20,21]. Saccharides and sulfated glycosaminoglycans have been shown to bind to Aβ and interfere with fibril formation [22,23]. However their role in fibril formation is controversial. Negatively charged saccharides are generally described as Aβ aggregation promoters but low molecular weight saccharides and glycosaminoglycans can also be neuroprotective. The glucosidic moiety in piceid, a resveratrol analog appeared as an important determinant of its Aβ disaggregation activity [11,24]. However, to the best of our knowledge, sugar-based peptidomimetics have not yet been described as inhibitors of amyloid formation.

Four peptidomimetic molecules (Fig. 1) differing by the length of the linker in position 1 ($n = 2, 3$) and the anomeric carbon configuration (α or β) were synthesized. These molecules were shown to decrease the rate of Aβ fibril formation by a fluorescence thioflavin-T binding assay and transmission electron microscopy. The conformation of these molecules and their interaction properties with Aβ were investigated by NMR spectroscopy.

2. Results and discussion

2.1. Chemistry

The synthesis of compounds **1**–**4** is described in Scheme 1. The intermediate **8** was prepared from the commercially available methyl-α-D-glucopyranoside **5** by successive tritylation of the primary hydroxyl in C6, benzylation of the three hydroxyls in C2, C3 and C4 and then hydrolysis of the trityl protection of **7** [25,26]. A Michael addition of **8** on *tert*-butylacrylate was carried out in the presence of a catalytic amount of tetrabutyl ammonium bromide

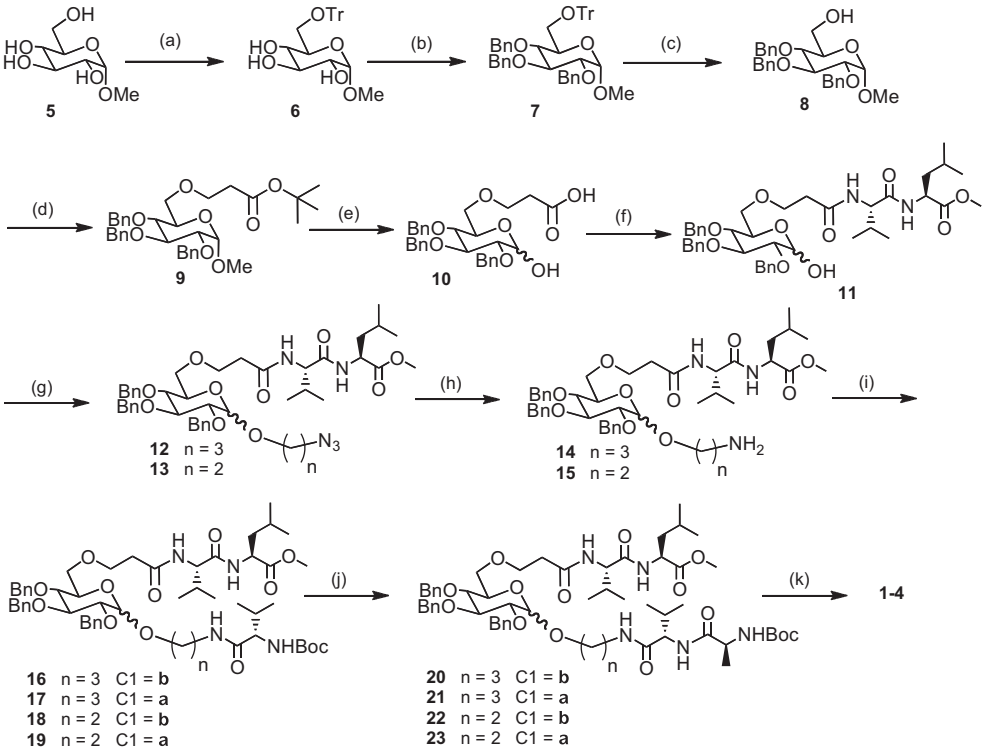

Scheme 1. Synthesis of peptidomimetics **1**–**4**. Reagents and conditions: a) TrCl, Et_3N, DMF, rt, 92%. b) BnBr, NaH, DMF, rt, 75%. c) *p*-TsOH, MeOH/CH_2Cl_2, rt, 70%. d) *tert*-butylacrylate, TBAB (15% m/m), 20% aqueous NaOH, rt, 90%. e) CF_3SO_3H, H_2O, AcOH, 80 °C, 55%. f) H–Val-Leu–OMe, HBTU, HOBt, DIPEA, DMF, rt, 94%. g) Cl_3CCN, NaH, CH_2Cl_2, rt then azidoalcohol, $BF_3{\cdot}OEt_2$, CH_2Cl_2, −20 °C, 59%, ratio α:β = 1:1 for **12** and 49%, ratio α:β = 1:1 for **13**. h) PPh_3, THF/H_2O, rt, 78% for **14** and 76% for **15**. i) *N*-Boc–L-Val, HBTU, HOBt, DIPEA, DMF, rt, then epimers separation by gel chromatography, 91% (α:β = 40:60) for **16**–**17** and 85% (α:β = 45:55) for **18**–**19**. j) TFA, CH_2Cl_2, rt, 100% then *N*-Boc-L-Ala, HBTU, HOBt, DIPEA, DMF, rt, 68% for **20**, 88% for **21**, 76% for **22**, and 75% for **23**. k) H_2, $Pd(OH)_2$, CH_2Cl_2/MeOH, 100% for **1**, 92% for **2**, 96% for **3** and 89% for **4**.

(TBAB) and in a 20% aqueous sodium hydroxide solution to introduce, in good yield (90%), a carboxy ethyl link on the primary hydroxyl group in C6 (compound **9**, Scheme 1) [27,28].

The C1 methoxy group and the *tert*-butyl ester were cleaved by a trifluorosulfonic acid solution in acetic acid at 80 °C [29] in 55% yield (ratio α:β = 1:1), and the obtained product **10** was coupled with the dipeptide H–Val-Leu–OMe using classical coupling reagents (HBTU, HOBt) to give the intermediate compound **11** in excellent yield (94%). Addition of compound **11** on trichloroacetonitrile using NaH as a base, provided the α-imidate according to the literature and to the ^{1}H NMR spectrum (H_1: $\delta = 6.35$ ppm and $J_{1,2} = 3$ Hz) [30]. Nucleophilic substitution reactions by azidopropanol (prepared from bromopropanol [31]) and by azidoethanol (prepared from bromoethanol [32]) as glycosyl acceptors were carried out with $BF_3 \cdot OEt_2$ as Lewis acid at −20 °C [30,33] to provide **12** and **13** respectively in 59% and 49% yield for the two steps from **11**. These "Schmidt" conditions [33] are described to yield essentially the β-isomer [30]. However, in our case, the α and β epimers of **12** and **13** were obtained in equal proportion and could not be separated at this stage. The peptidic chain in C6 could maybe interfere during the mechanism of nucleophilic substitution of the azidoalcohol and prevent

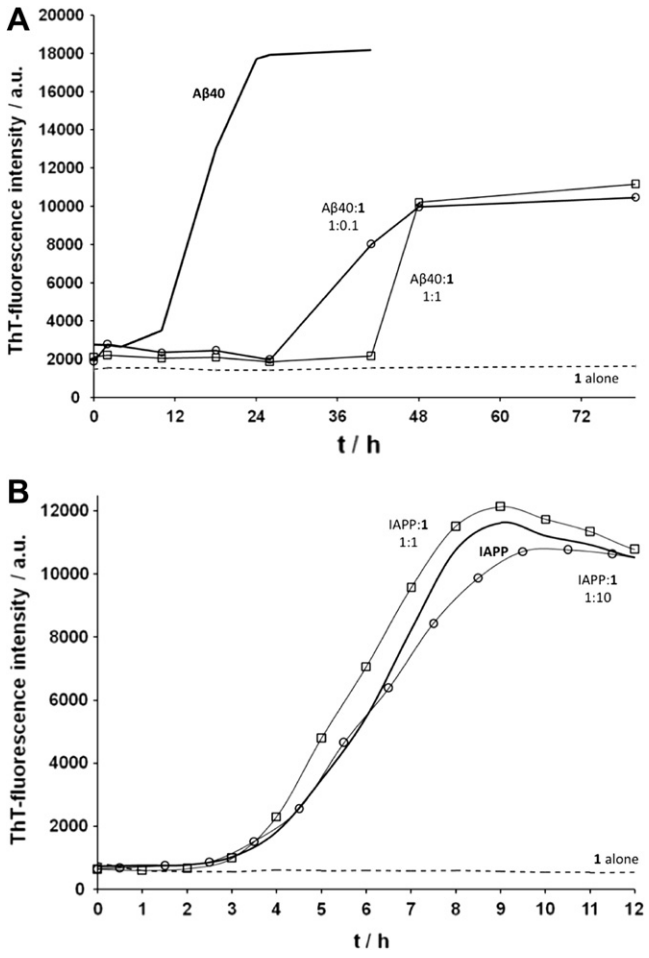

Fig. 2. (A) Representative ThT fluorescence assay showing the fibril formation of $A\beta_{1-40}$ in the absence (solid) or in the presence of the peptidomimetic **1** at a Aβ:peptidomimetic ratio of 1:0.1 (solid with open circle) and 1:1 (solid with open square). ThT traces are shown for peptidomimetic **1** alone (dash). (B) Representative ThT fluorescence assay showing the fibril formation of IAPP in the absence (solid) or in the presence of the peptidomimetic **1** at a Aβ:peptidomimetic ratio of 1:1 (solid with open square) and 1:10 (solid with open circle). ThT traces are shown for peptidomimetic **1** (dash).

Table 1
Inhibition of $A\beta_{1-40}$ fibrillation by sugar-based peptidomimetics **1**–**4** at a 1:1 Aβ:peptidomimetic ratio.

Compound	Lag extension (fold increase)[a]	Plateau reduction (% inhibition)[a]
1	3.0 ± 1.0	52 ± 15
2	3.4 ± 1.0	60 ± 15
3	3.4 ± 1.0	40 ± 15
4	3.4 ± 1.0	22 ± 10

[a] Parameters are expressed as mean ± SE, $n = 2$–6 (see Experimental section for the calculation of the lag extension of the plateau reduction).

a stereoselective reaction. However, we were interested in both isomers so we pursued the following synthetic steps. The azido group of **12** and **13** was reduced via a Staudinger reaction in 78% and 76% yields respectively. The obtained amines **14** and **15** were coupled with *N*-Boc–L-Val, using HBTU and HOBt as coupling reagents, to afford after separation of α and β isomers compounds **16** and **17** in 56% and 35% yields respectively, and compounds **18** and **19** in 45% and 40% yields respectively. The rest of the synthesis was carried out separately for the two α and β isomers. The Boc groups were cleaved by TFA in quantitative yield and the free amines were coupled with *N*-Boc–L-Ala using HBTU and HOBt as coupling reagents to obtain compounds **20** and **21** in 68% and 88% yields respectively from **16** and **17**, and to obtain compounds **22** and **23** in 76% and 75% yields respectively from **18** and **19**. Finally, the cleavage of benzyl groups by catalytic hydrogenation using $Pd(OH)_2$ as catalyst afforded the desired final compounds **1**, **2**, **3** and **4** in 100%, 92%, 96% and 89% yields, respectively.

2.2. Fluorescence spectroscopy

The ability of compounds **1**–**4** to inhibit amyloid fibril formation was first tested on $A\beta_{1-40}$ peptide. The fluorescence-detected thioflavin-T (ThT) binding assay is the standard method used to monitor the time course of fibril formation [34]. The final ThT fluorescence intensity is dependent on the amount of fibrillar material formed, the binding constant for ThT, and the quantum yield of the bound dye. The fluorescence assay of $A\beta_{1-40}$ at a concentration of 20 μM shows a typical fibrillation process with a lag phase of approximately 12 h followed by a growth phase and a final plateau (Fig. 2A).

Fig. 2A shows that peptidomimetic **1** at $A\beta_{1-40}$:**1** ratios of 1:0.1 and 1:1 increases the lag phase of $A\beta_{1-40}$ from 12 to 26 and 41 h respectively. In addition, the final fluorescence intensity is significantly reduced relative to $A\beta_{1-40}$ alone by a factor of 2 (Fig. 2A). Control experiments indicate that, under the experimental conditions used, the ThT fluorescence of the peptidomimetic remains low (Fig. 2A, dash dot). Similar results were observed with peptidomimetics **2**–**4**, namely a reduction of fibril formation accompanied by an increase in the lag time. The results for all peptidomimetics are summarized in Table 1 with respect to their effect upon both lag extension and equilibrium plateau reduction. All compounds exhibit strong inhibitory capabilities, increasing the

Table 2
Effects on IAPP fibrillation induced by sugar-based peptidomimetics **1**–**4** at a 1:10 IAPP:peptidomimetic ratio.

Compound	Lag extension (fold increase)[a]	Plateau reduction (% inhibition)[a]
1	1	5 ± 5
2	1	9 ± 5
3	1	1 ± 4
4	Slight promotion	Slight promotion

[a] Parameters are expressed as mean ± SE, $n = 6$ (see Experimental section for the calculation of the lag extension of the plateau reduction).

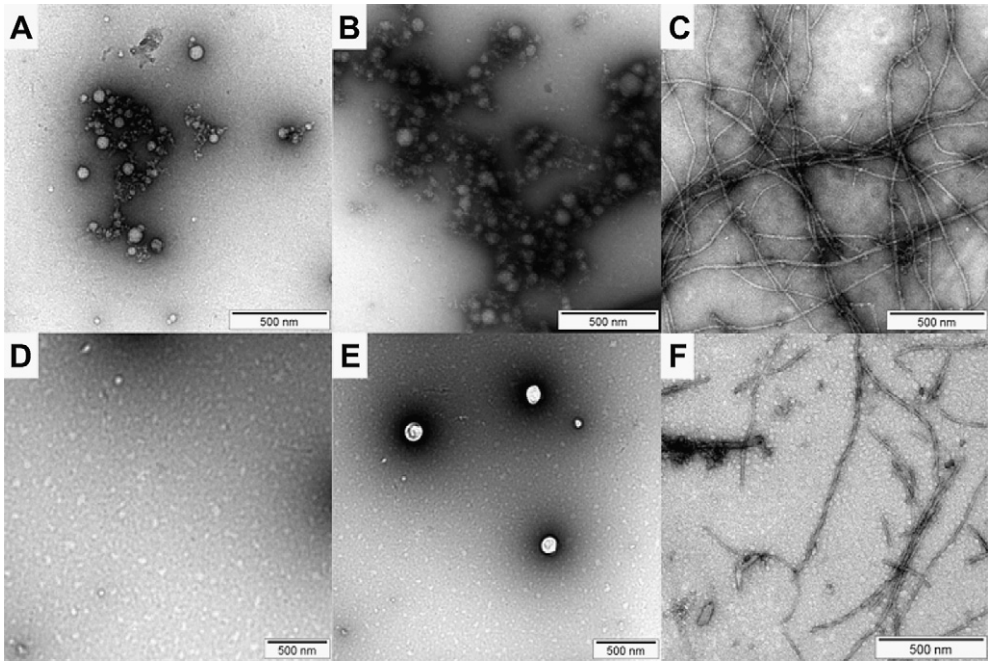

Fig. 3. Negatively stained electron microscopy images of fibril formation of $A\beta_{1-40}$alone (top) and in the presence of the peptidomimetic **1** (down) at a 1:1 ratio in 10 mM Tris·HCl, 100 mM NaCl buffer at pH 7.4 after 1 day (A and D), 2 days (B and E) and 2 weeks of incubation (C and F). Panel F shows the rare isolated fibrils observed (scale bars, 500 nm).

lag time by a factor of approximately 3 and reducing the equilibrium plateau by 20–60%. These results indicate that the peptidomimetics inhibit $A\beta_{1-40}$ fibril formation but that the length of the aminoalkyl link and the configuration of the anomeric center have only little influence on these inhibition properties.

Next, we wanted to investigate if the inhibition effect observed on $A\beta_{1-40}$ was specific. For that purpose, the effects on another amyloid peptide, IAPP (Islet Amyloid Polypeptide), involved in type II diabetes mellitus were evaluated [35]. This peptide shares similar features in length (37 residues), sequence (~20% identity) and morphology of amyloid fibrils. Fluorescence data show a fast fibrillation process for IAPP (5 μM) with a lag phase of ~3 h in agreement with previous results [36].

However, the peptidomimetics **1**–**4** do not inhibit the IAPP fibril formation even at a high IAPP:peptidomimetic ratio of 1:10 (Fig. 2B and Table 2). The lag time is not reduced after addition of the peptidomimetics and the final fluorescence intensity remains the same. In addition, our results show that peptidomimetic **4** slightly promotes aggregation as evidenced by a decrease in the lag time and an increase in the equilibrium plateau relative to the control. Overall, our data demonstrate that the peptidomimetics **1**–**4** do not inhibit IAPP fibril formation, whereas they are potent inhibitors of $A\beta_{1-40}$ fibrillation even at low ratios of inhibitors.

2.3. Transmission electron microscopy

The reduction of the final fluorescence intensity of $A\beta_{1-40}$ induced by the peptidomimetics should not necessarily be interpreted in terms of the amount of amyloid formed. Indeed, the changes in the binding constant or the quantum yield of the dye can also contribute to any observed differences. Thus, this is critical to assay any potential inhibitors by an independent method. Transmission electron microscopy (TEM) studies conducted as a function of time confirm that the peptidomimetics significantly affect $A\beta_{1-40}$ fibril formation but do not affect IAPP fibril formation. Aliquots of each reaction mixture were collected at different time points, and TEM images recorded. After 1–2 days, TEM images of $A\beta_{1-40}$ show small and large spherical aggregates (Fig. 3A and B), while after 2 weeks TEM images reveal dense mats of fibrils with the classical morphology (Fig. 3C). In contrast, images of $A\beta_{1-40}$:**1** mixture at a 1:1 ratio, collected after 1 and 2 days show almost no aggregates (Fig. 3D–E). In addition, after 2 weeks of incubation, very few fibrils are observed. The population of $A\beta_{1-40}$:**1** mixture fibrillar assemblies consists of thin fibrils that, in contrast with $A\beta_{40}$ alone, do not appear to have a strong propensity to cluster. (Fig. 3F). Similar results were observed with $A\beta_{1-40}$:**1** at a 1:0.1 ratio (data not shown).

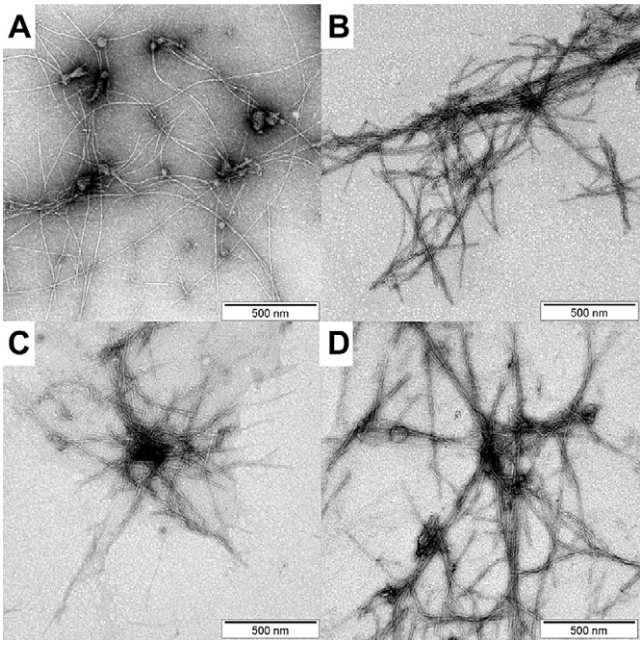

Fig. 4. Negatively stained electron microscopy images of fibril formation of IAPP alone (top) and in the presence of the peptidomimetic **1** (down) at a 1:10 ratio in 10 mM Tris·HCl, 100 mM NaCl buffer at pH 7.4 after 3 h (A and C) and 24 h of incubation (B and D) (scale bars, 500 nm).

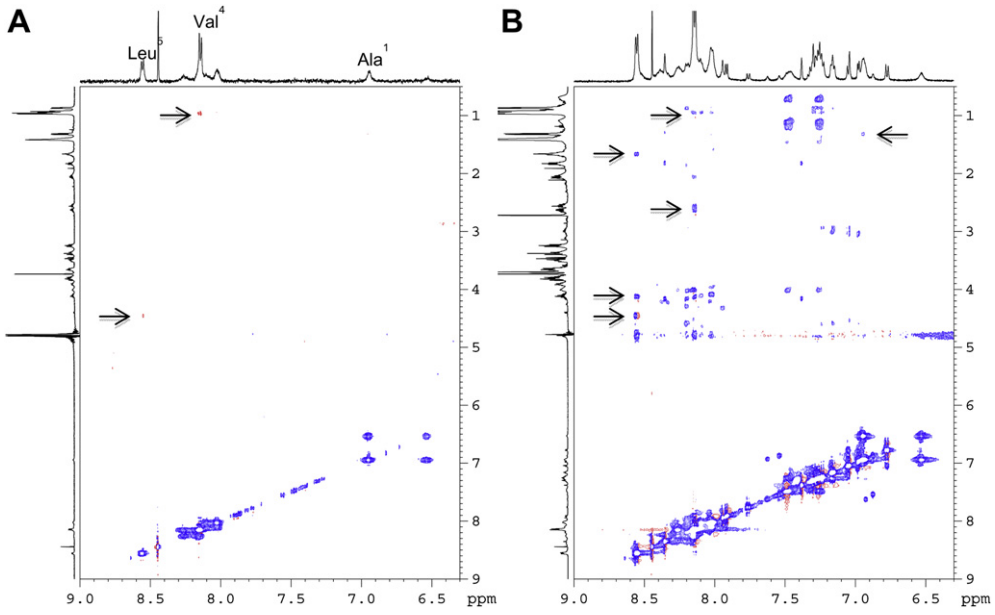

Fig. 5. 2D NOESY spectra of peptidomimetic **1** in the absence (A) and in the presence (B) of $A\beta_{1-40}$. Positive signals are shown with blue contour levels and negative signals with red contour levels. NOE correlations indicated by arrows correspond to intramolecular NOEs of peptidomimetic **1**. (For interpretation of the references to color in this figure legend, the reader is referred to the web version of this article.)

Next, TEM images of IAPP alone and IAPP:**1** mixture at a 1:10 ratio were collected after 3 and 24 h. In both cases with and without the peptidomimetic, the images reveal dense mats of fibrils with the classical morphology (Fig. 4A–D). Our data demonstrate that the peptidomimetics dramatically slow down the aggregation of $A\beta_{1-40}$ and efficiently reduce the amount of typical amyloid fibrils, whereas they do not affect the kinetics of IAPP fibril formation neither decrease the amount of IAPP fibrils.

2.4. NMR spectroscopy

NMR studies carried out in aqueous solution showed that peptidomimetics **1**–**4** are highly soluble in water and are not prone to aggregation, as indicated by the observation of small proton resonance line widths and the absence of significant chemical shift dependency upon concentration variation (0.25–2.8 mM range). The analysis of chemical shifts, vicinal coupling constants and ROEs shows that the linker segments and the dipeptide units are highly flexible in solution. The amide protons exhibit large temperature dependency of their chemical shifts (−10.1 to −6.4 ppb/°C) suggesting that they are not sequestered from solvent. The large $^3J_{HN,H\alpha}$ coupling constants (≥7.5 Hz) of Val and Leu residues suggest that extended conformations are significantly populated for these hydrophobic residues. This is also confirmed by the analysis of intraresidual and sequential Hα–HN ROEs. The temperature coefficients and the absence of long-range ROEs indicate that peptidomimetics alone do not form stable β-sheets either intramolecularly or intermolecularly.

Since these peptidomimetics showed very similar results in terms of conformation and inhibition properties, a single peptidomimetic was selected for further NMR studies in aqueous solution in the presence of $A\beta_{1-40}$. 1D and 2D NMR experiments realized on different mixtures of peptidomimetic **1** and $A\beta_{1-40}$ did not show significant chemical shift changes of peptidomimetic resonances. It has been shown that the NMR spectrum of $A\beta_{1-40}$ is dominated by the monomeric species, the oligomeric and fibril species being NMR-invisible [37]. In our case, we did not observe any significant chemical shift changes of $A\beta_{1-40}$ resonances upon addition of peptidomimetic **1**. These results tend to indicate that peptidomimetic **1** does not strongly interact with monomeric $A\beta_{1-40}$ peptide.

However the 2D NOESY spectra of peptidomimetic **1** (1 mM) showed significant differences in NOEs upon addition of $A\beta_{1-40}$ peptide (0.25 mM). Indeed, while the NOE correlations are characterized by positive or near zero values in the absence of $A\beta_{1-40}$, the addition of $A\beta_{1-40}$ leads to the appearance of negative NOEs for the HN/aliphatic protons correlations of peptidomimetic **1** (Fig. 5).

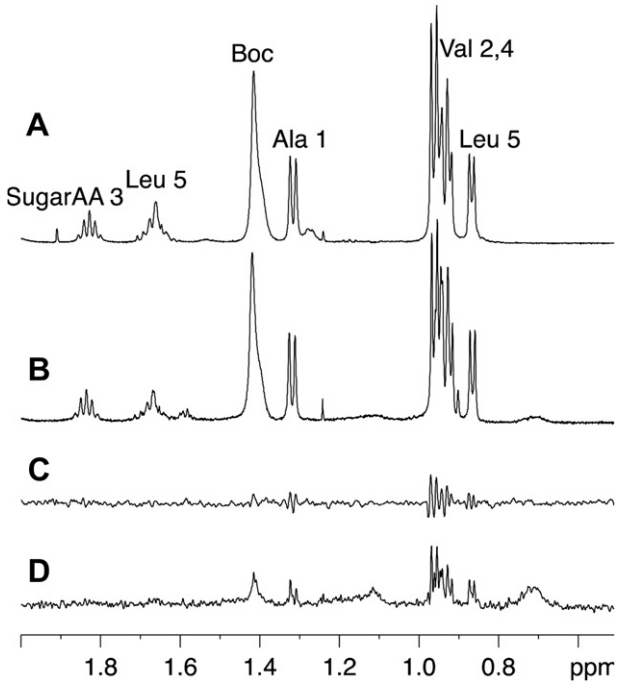

Fig. 6. (A and B) Aliphatic region of 1D ^{1}H NMR spectra of peptidomimetic **1** (0.6 mM) alone (A) and in the presence of 30 μM $A\beta_{1-40}$ (B). (C and D) 1D STD spectra of the mixture of peptidomimetic **1** (0.6 mM) and $A\beta_{1-40}$ (30 μM) recorded after a period of 1 h (C) and 2 weeks (D). The dispersion peaks observed in (C) are difference artefacts.

The detection of negative NOE correlations clearly indicates that peptidomimetic **1** is able to interact with $A\beta_{1-40}$ species. In the absence of chemical shift modifications of $A\beta_{1-40}$ resonances, as aforementioned, we postulate that the negative transferred NOEs arise from the interaction with aggregated, NMR-invisible $A\beta_{1-40}$ species.

To confirm this hypothesis, the interaction of peptidomimetic **1** with $A\beta_{1-40}$ was further examined by saturation transfer difference (STD) experiments [38] at different concentrations. No STD signal was observed on peptidomimetic **1** alone (1 mM concentration). In the presence of $A\beta_{1-40}$ (0.25 mM), STD signals were observed for the methyl resonances of Ala, Leu, and Val residues of peptidomimetic **1**, proving that **1** interacts with $A\beta_{1-40}$ species through its hydrophobic amino acids. Similar experiments were carried out at lower concentrations of $A\beta_{1-40}$ (30 μM) corresponding to an $A\beta_{1-40}$:**1** ratio of 1:20. STD signals were not observed initially (Fig. 6C), indicating that the aggregated species of $A\beta_{1-40}$ interacting with peptidomimetic **1** were not present at the very beginning in these diluted $A\beta_{1-40}$ samples. However the STD signals were observed after a period of about 2 weeks (Fig. 6D). This time dependence of STD signal can be explained by the slow conversion of monomeric $A\beta_{1-40}$ to aggregated species and confirms that peptidomimetic **1** interacts preferentially with aggregated $A\beta_{1-40}$ species.

3. Conclusions

In summary, we have described a novel class of water-soluble aggregation inhibitors based on a flexible sugar amino acid inserted in the center of a short hydrophobic peptidic sequence to destabilize locally the β-sheet structure of Aβ aggregated species. These compounds combine the targeting of hydrophobic recognition interfaces with an original hydrophilic sugar β-breakage strategy. These peptidomimetics dramatically slow down the aggregation of $A\beta_{1-40}$ even at low concentrations (peptidomimetic to $A\beta_{1-40}$ ratios of 0.1:1) and efficiently reduce the amount of typical amyloid fibrils. Noteworthy, this inhibition effect is sequence-specific since these molecules do not alter the kinetics of aggregation of IAPP amyloid peptide. These peptidomimetics do not strongly interact with unordered/α-helix $A\beta_{1-40}$ monomer, as suggested by the absence of NMR chemical shift perturbation. This points toward a distinct mechanism of action from other inhibitors such as D-Trp-Aib, which was shown to interact with Aβ monomer using a similar NMR approach [19]. However, trNOEs and STD experiments revealed that these peptidomimetics are in dynamic equilibrium with complexes involving Aβ species. Therefore the inhibition effect probably results from binding to Aβ aggregated species. Further experiments are necessary to decipher the binding mode of these peptidomimetic inhibitors to $A\beta_{1-40}$ species and to analyze if the Aβ aggregation cascade is redirected toward off-pathway species [11].

4. Experimental

4.1. Chemistry

Usual solvents were purchased from commercial sources and dried and distilled by standard procedures. Azidopropanol was prepared from bromopropanol [31] and azidoethanol was prepared from bromoethanol [32] according to methods reported in the literature. H–Val-Leu–OMe was prepared according to classical literature reported coupling method using isobutyl-chloroformiate. Pure products were obtained after flash chromatography using Merck silica gel 60 (40–63 μm). TLC analyses were performed with 0.25 mm 60 F_{254} silica plates (Merck). Element analyses (C, H, N) were performed on a Perkin–Elmer CHN, Analyser 2400. Mass spectra were obtained using a Bruker Esquire electrospray ionization apparatus. IR spectra were recorded on a Bruker Vector 22 FT-IR spectrometer. NMR standard spectra were recorded on a Bruker AMX 200, (^{1}H, 200 MHz, ^{13}C, 50 MHz) or an Ultrafield AVANCE 300 (^{1}H, 300 MHz, ^{13}C, 75 MHz) or a Bruker AVANCE 400 (^{1}H, 400 MHz, ^{13}C, 100 MHz). Chemical shift δ are in parts per million and the following abbreviations are used: singlet (s), doublet (d), triplet (t), multiplet (m), broad singlet (br s).

4.1.1. Synthesis of peptidomimetics *1*–*4*

*4.1.1.1. Boc–Ala-Val-[(C1)β-glucose-(n3)]-Val-Leu–OMe **1**.* A solution of **20** (75 mg, 0.07 mmol) and $Pd(OH)_2$ (18 mg, mass 25%) in MeOH/DCM 3:1 (4 ml) was stirred under hydrogen atmosphere for 3 h then the mixture solution was filtered on Celite and evaporated under reduced pressure to afford **1** as a yellowish white solid (57 mg, 100%). IR (neat): $\nu = 3273$ (O–H), 2963 (N–H), 1645 (C=O), 1633 (C=O); MS (ESI, ion polarity positive): m/z: 828 $[M + Na]^+$; HRMS (TOF, ion polarity positive): calcd for $C_{37}H_{67}N_5O_{14}Na$: 828.4582; found: 828.4583. The NMR assignment is shown in Table S1 (Supplementary data).

*4.1.1.2. Boc–Ala-Val-[(C1)α-glucose-(n3)]-Val-Leu–OMe **2**.* A solution of **21** (143 mg, 0.13 mmol) and $Pd(OH)_2$ (36 mg, mass 25%) in MeOH/DCM 3:1 (6.6 ml) was stirred under hydrogen atmosphere for 3 h then the mixture solution was filtered on Celite and evaporated under reduced pressure to afford **2** as a white solid (99 mg, 92%). $C_{37}H_{67}N_5O_{14} + 2.25H_2O$: calcd C 52.50, H 8.51, N 8.27; found C 52.48, H 8.22, N 8.26; IR (neat): $\nu = 3273$ (O–H), 3034 (N–H), 2963 (N–H), 1645 (C=O), 1633 (C=O); MS (ESI, ion polarity positive): m/z: 828 $[M + Na]^+$; HRMS (TOF, ion polarity positive): calcd for $C_{37}H_{67}N_5O_{14}Na$: 828.4582; found: 828.4583. The NMR assignment is shown in Table S2 (Supplementary data).

*4.1.1.3. Boc–Ala-Val-[(C1)β-glucose-(n2)]-Val-Leu–OMe **3**.* A solution of **22** (126 mg, 0.12 mmol) and $Pd(OH)_2$ (32 mg, mass 25%) in MeOH/DCM 3:1 (6 ml) was stirred at rt, under hydrogen atmosphere for 4 h. The mixture solution was filtered on Celite and the filtrate was evaporated under reduced pressure to afford **3** as a white solid (99 mg, 96%); m.p. decomposition; $C_{36}H_{65}N_5O_{14} + 2.0H_2O$: calcd C 52.22, H 8.40, N 8.46; found C 52.20, H 7.78, N 8.20; IR (neat): $\nu = 3279$ (O–H), 2957 (N–H), 1635 (C=O); MS (ESI, ion polarity positive): m/z: 814 $[M + Na]^+$; HRMS (TOF ESI, ion polarity positive): calcd for $C_{36}H_{65}N_5O_{14}Na$: 814.4426; found: 814.4395. The NMR assignment is shown in Table S3 (Supplementary data).

*4.1.1.4. Boc–Ala-Val-[(C1)α-glucose-(n2)]-Val-Leu–OMe **4**.* A mixture of **23** (105 mg, 0.1 mmol) and $Pd(OH)_2$ (27 mg, mass 25%) in MeOH/DCM 3:1 (5 ml) was stirred at rt, under hydrogen atmosphere for 4 h. The mixture solution was then filtered on Celite and the filtrate was evaporated under reduced pressure to afford **4** as a white solid (70 mg, 89%); m.p. decomposition; $C_{36}H_{65}N_5O_{14} + 2.0H_2O$: calcd C 52.22, H 8.40, N 8.46; found C 51.92, H 7.68, N 8.04; IR (neat): $\nu = 3295$ (O–H), 2971 (N–H), 1641 (C=O); MS (ESI, ion polarity positive): m/z: 814 $[M + Na]^+$; HRMS (TOF ESI, ion polarity positive): calcd for $C_{36}H_{65}N_5O_{14}Na$: 814.4426; found: 814.4435. The NMR assignment is shown in Table S4 (Supplementary data).

4.1.2. Synthesis of intermediates *6*–*15*

*4.1.2.1. Methyl 6-O-(triphenylmethyl)-α-D-glucopyranoside **6**.* A solution of methyl-α-D-glucopyranoside **5** (1.0 g, 5.2 mmol), trityl chloride (1.5 g, 5.7 mmol) and triethylamine (1.3 ml, 9.3 mmol) in dry DMF (15 ml) was stirred overnight at room temperature under nitrogen. After 24 h, the solvent was evaporated under reduced

pressure and the residue was dissolved in EtOAc (20 ml) and water (20 ml). After the separation of the layers, aqueous layer was extracted with EtOAc (3 × 10 ml). The combined organic layers were dried with $MgSO_4$, filtered and evaporated under reduced pressure. The crude residue was purified by chromatography on a silica gel column (cyclohexane/EtOAc, 4:6 then 2:8) to give compound **6** as a white solid (2.1 g, 92%). ^{1}H NMR (400 MHz, $CDCl_3$, 25 °C): $\delta = 7.47-7.30$ (m, 15H, H_{arom}), 4.71 (d, ^3J(H, H) = 3.6 Hz, 1H, $H_{1\beta}$), 3.68 (m, 1H, H_5), 3.65 (dd, ^3J(H, H) = 3.6, 9.1 Hz, 1H, H_2), 3.45 (t, ^3J(H, H) = 9.1 Hz, 1H, H_3), 3.39 (m, 3H, OCH_3), 3.37 (m, 1H, H_4), 3.31 (m, 2H, H_6); ^{13}C NMR (100 MHz, $CDCl_3$, 25 °C): δ = 143.9, 128.7, 127.8, 127.0, 99.2, 86.7, 74.4, 72.0, 71.3, 70.4, 63.9, 55.0; m.p. 153–155 °C (lit. [39]: m.p. 154.5–155.5 °C); IR (neat): $\nu = 3429$ (O–H); $C_{26}H_{29}O_6$: calcd C 71.54, H 6.47; found: C 71.35, H 6.42; MS (ESI, ion polarity positive): m/z: 459 $[M + Na]^+$.

4.1.2.2. Methyl 2,3,4-tri-O-benzyl-6-O-(triphenylmethyl)-α-D-glucopyranoside ***7***. To a solution of **6** (1.41 g, 3.22 mmol) in DMF (15 ml) were added NaH (970 mg, 24.2 mmol) and benzyl bromide (2.4 ml, 19.3 mmol). The reaction mixture was stirred at rt overnight. Excess of NaH was destroyed by addition of MeOH (20 ml) and water (10 ml). MeOH was evaporated under reduced pressure and DCM (10 ml) was added. After the separation of the layers, the aqueous layer was extracted with DCM (2 × 5 ml). The combined organic layers were dried over $MgSO_4$, filtered and evaporated under reduced pressure. The crude residue was purified by chromatography on a silica gel column (cyclohexane/EtOAc, 4:6 then 2:8) to afford compound **7** as a colorless oil (1.71 g, 75%). ^{1}H NMR (400 MHz, $CDCl_3$, 25 °C): $\delta = 7.57-6.95$ (m, 30H, H_{arom}), 5.04–4.77 (m, 7H, 3 × PhCH_2 and $H_{1\beta}$), 4.07 (m, 1H, H_3), 3.91 (m, 1H, H_5), 3.73 (m, 2H, H_4, H_2), 3.61 (m, 1H, H_6), 3.54 (s, 3H, OCH_3), 3.29 (m, 1H, H_6); ^{13}C NMR (100 MHz, $CDCl_3$, 25 °C): δ = 143.9, 138.8, 138.3, 138.0, 128.8, 128.4, 128.3, 128.1, 128.0, 127.9, 127.7, 127.6, 127.4, 127.1, 126.9, 126.2, 97.9, 86.3, 82.3, 80.3, 78.2, 75.9, 74.9, 73.3, 70.3, 62.7, 54.9; IR (neat): $\nu = 3080$ (C_{arom}–H); 3030 (C_{arom}–H); 1069 (C–O); 1028 (C–O); MS (ESI, ion polarity positive, MeOH): m/z: 729 $[M + Na]^+$.

4.1.2.3. Methyl 2,3,4-tri-O-benzyl-α-D-glucopyranoside ***8***. A solution of **7** (1.75 g, 2.48 mmol) and *p*-TsOH (50 mg, 0.26 mmol) in DCM/MeOH 1:2 (25 ml) was stirred overnight. Then the solvent was evaporated under reduced pressure and the crude residue was dissolved with DCM (10 ml). This solution was washed with water (2 × 10 ml), aqueous 10% Na_2CO_3 solution (10 ml) and aqueous saturated NaCl solution (10 ml). The organic layer was dried over $MgSO_4$, filtered and evaporated under reduced pressure. The crude residue was purified by chromatography on a silica gel column (cyclohexane/AcOEt, 7:3 then 6:4) to afford **8** as white solid (806 mg, 70%). ^{1}H NMR (400 MHz, $CDCl_3$, 25 °C): $\delta = 7.30-7.42$ (m, 15H, H_{arom}), 5.02 (d, ^3J(H, H) = 11.0 Hz, 1H, H_{15}), 4.92–4.82 (m, 6H, 3 × PhCH_2), 4.60 (d, ^3J(H, H) = 3.0 Hz, 1H, $H_{1\beta}$), 4.04 (t, ^3J(H, H) = 9.0 Hz, 1H, H_3), 3.67–3.78 (m, 3H, H_5, H_6), 3.52–3.58 (m, 2H, H_2, H_4), 3.39 (s, 3H, OCH_3); ^{13}C NMR (100 MHz, $CDCl_3$, 25 °C): δ = 138.7, 138.1, 138.1, 128.4, 128.3, 128.0, 127.9, 127.9, 127.8, 127.5, 98.1, 81.9, 79.9, 77.4, 75.7, 74.9, 73.3, 70.7, 61.7, 55.1; m.p. 187–189 °C; IR (neat): $\nu = 3467$ (O–H); $C_{28}H_{32}O_6$: calcd C 72.39, H 6.94; found C 72.39, H 7.17; MS (ESI, ion polarity positive, MeOH): m/z: 487 $[M + Na]^+$.

4.1.2.4. Methyl 6-O-[2-(carboxy-tert-butyl)ethyl]-2,3,4-tri-O-benzyl-α-D-glucopyranoside ***9***. To a suspension of **8** (5.0 g, 10.8 mmol) in *tert*-butylacrylate (3.13 ml, 21.6 mmol) were added TBAB (0.52 g, 1.62 mmol) and a 20% aqueous solution of sodium hydroxide (47 ml). The reaction mixture was stirred for 4 h then water (100 ml) and EtOAc (100 ml) were added. The different layers were separated and the aqueous layer was extracted with EtOAc (2 × 100 ml). The combined organic layers were dried over $MgSO_4$, filtered and evaporated under reduced pressure. The crude residue was purified by chromatography on a silica gel column (cyclohexane/EtOAc, 8:2) to afford compound **9** as a colorless oil (5.49 g, 90%). ^{1}H NMR (400 MHz, $CDCl_3$, 25 °C): $\delta = 7.23-7.17$ (m, 15H, H_{arom}), 4.88–5.51 (m, 7H, 3 × PhCH_2 and $H_{1\beta}$), 3.88 (t, ^3J(H, H) = 10.0 Hz, 1H, H3), 3.60–3.43 (m, 7H, H_2, H_4, H_5, H_6, OCH_2), 3.35 (s, 3H, OCH_3), 2.38 (m, 2H, CH_2–CO), 1.31 (s, 9H, CH_3–Boc); ^{13}C NMR (100 MHz, $CDCl_3$, 25 °C): δ = 138.6, 138.2, 137.9, 128.1, 128.0, 127.8, 127.7, 127.6, 127.4, 127.3, 97.9, 81.8, 80.2, 79.6, 77.3, 75.4, 74.7, 73.1, 69.8, 69.2, 66.9, 54.8, 35.9, 27.8; IR (neat): $\nu = 1731$ (C=O); $C_{35}H_{34}O_8$: calcd C 70.92, H 7.48; found C 70.96, H 7.45; MS (ESI, ion polarity positive, MeOH): m/z: 616 $[M + Na]^+$.

4.1.2.5. 6-O-[2-(carboxyethyl)]-2,3,4-tri-O-benzyl-α-D-glucopyranoside ***10***. To a solution of **9** (1.2 g, 2.02 mmol) in acetic acid (23 ml) was added a solution of 2 N trifluorosulfonic acid (4.0 ml, 8.08 mmol). The reaction mixture was stirred for 5 h at 80 °C then water (20 ml) and DCM (30 ml) were added. The different layers were separated and the aqueous layer was extracted with EtOAc (4 × 20 ml). The combined organic layers were dried over $MgSO_4$, filtered and evaporated under reduced pressure. The crude residue was purified by chromatography on a silica gel column (cyclohexane/EtOAc/AcOH, 8:2:0 then 20:75:5) to afford compound **10** as a yellowish oil (2.0 g, 55%, ratio α:β = 1:1). ^{1}H NMR (400 MHz, $CDCl_3$, 25 °C): $\delta = 7.40-7.25$ (m, 15H, H_{arom}), 5.16 (d, ^3J(H, H) = 3.5 Hz, 0.5H, $H_{1\alpha}$), 4.99–4.57 (m, 6.5H, $H_{1\beta}$ and 3 × PhCH_2), 3.96 (m, 1H, H_3), 3.65–3.31 (m, 6H, H_2, H_4, H_5, H_6, OCH_2), 2.51 (t, ^3J(H, H) = 6.2 Hz, 2H, CH_2–CO); ^{13}C NMR (100 MHz, $CDCl_3$, 25 °C): δ = 176.3, 176.1, 138.7, 138.5, 138.4, 138.3, 138.1, 137.9, 128.5, 128.5, 128.2, 128.1, 128.0, 128.0, 127.8, 127.7, 97.5, 91.2, 84.5, 83.2, 81.7, 80.0, 75.8, 75.0, 74.8, 74.3, 73.2, 70.0, 69.9, 66.6, 66.6, 34.7; IR (neat): $\nu = 3369$ (O–H), 1719 (C=O); $C_{30}H_{34}O_8 + 0.34H_2O$: calcd C 68.15, H 6.61; found C 68.16, H 6.74; MS (ESI, ion polarity positive, MeOH): m/z: 545 $[M + Na]^+$.

4.1.2.6. Synthesis of compound ***11***. To a solution of **10** (1.8 g, 3.44 mmol) in DMF (25 ml) were added HBTU (1.83 g, 4.82 mmol), HOBt (0.65 g, 4.82 mmol), DIPEA (3 ml, 17.2 mmol) and H–Val-Leu–OMe (1.71 g, 4.82 mmol). The reaction mixture was stirred overnight at rt then the solvent was removed under reduced pressure and the residue was dissolved in EtOAc. This organic layer was washed with water (25 ml), an aqueous 10% citric acid solution (25 ml), an aqueous saturated $NaHCO_3$ solution (25 ml) and brine (25 ml). The organic layer was dried over $MgSO_4$, filtered and evaporated under reduced pressure. The crude residue was purified by chromatography on a silica gel column (cyclohexane/EtOAc, 2:8 then 0:10) to afford the desired product **11** as a yellowish solid (2.43 g, 94%). ^{1}H NMR (300 MHz, $CDCl_3$, 25 °C): $\delta = 7.99$ (m, 1H, NH), 7.65 (m, 1H, NH), 7.39–7.26 (m, 15H, H_{arom}), 6.69 (m, 1H, NH), 5.23–4.52 (m, 8H, H_1, 3 × PhCH_2 and CH_α–Leu), 4.25–4.12 (m, 2H, H_3 and CH_α–Val), 3.86–3.19 (m, 10H, H_2, H_4, H_5, H_6, OCH_2 and OCH_3), 2.53 (m, 2H, CH_2–CO), 2.03 (m, 1H, CH_β–Val), 1.62–1.58 (m, 3H, $CH_{2\beta}$–Leu and CH_γ–Leu), 0.95–0.85 (m, 12H, CH_3–Val and CH_3–Leu); ^{13}C NMR (75 MHz, $CDCl_3$, 25 °C): δ = 174.9, 172.7, 172.0, 138.6, 138.0, 128.6, 128.4, 128.1, 128.0, 127.9, 127.9, 127.8, 127.7, 98.1, 97.0, 92.1, 91.1, 84.6, 84.1, 83.3, 82.8, 81.2, 75.4, 75.1, 74.9, 74.8, 74.4, 70.8, 70.9, 68.8, 68.1, 66.2, 66.1, 65.7, 59.0, 58.9, 58.7, 52.3, 50.9, 41.0, 36.4, 29.9, 26.9, 21.9, 19.2, 18.7, 18.6; m.p. 136–138 °C; IR (neat): $\nu = 3273$ (O–H), 3034 (N–H), 2963 (N–H), 1745 (C=O), 1633 (C=O); $C_{42}H_{56}N_2O_{10}$: calcd C 67.36, H 7.54, N 3.74; found C 67.16, H 7.66, N 3.43; MS (ESI, ion polarity positive): m/z: 771 $[M + Na]^+$; HRMS (TOF ESI, ion polarity positive): calcd for $C_{42}H_{56}N_2O_{10}Na$: 771.3833; found: 771.3841.

4.1.2.7. Synthesis of compound ***12***. To a solution of **11** (805 mg, 1.1 mmol) in DCM (5 ml) were added successively NaH (56 mg, 1.4 mmol) and trichloroacetonitrile (931 mg, 6.5 mmol). The

reaction mixture was stirred 3 h at rt then the solvent was removed under reduced pressure and the residue was dissolved in DCM (7 ml). Azidopropanol (131 mg, 1.3 mmol) and $BF_3{\cdot}OEt_2$ (153 mg, 1.1 mmol) were added and the reaction mixture was stirred 3 h at −20 °C then quenched by addition of ice. The quenched reaction was extracted by DCM and the organic layer was washed by water (1 ml), an aqueous 5% $NaHCO_3$ solution (1 ml) and brine (1 ml). The organic layer was dried over $MgSO_4$, filtered and evaporated under reduced pressure. The crude residue was purified by chromatography on a silica gel column (DCM/OEt_2, 8:2) to afford the desired product **12** as a colorless oil (531 mg, 59%, ratio α:β = 1:1). ^{1}H NMR (400 MHz, $CDCl_3$, 25 °C): δ = 7.34–7.26 (m, 15H, H_{arom}), 6.69 (d, ^3J(H, H) = 8.9 Hz, 1H, *NH*–Val), 6.30 (d, ^3J(H, H) = 8.2 Hz, 1H, *NH*–Leu), 5.00–4.52 (massif, 7.5H, $H_{1\beta}$, 3 × Ph*CH*$_2$, C*H*$_\alpha$–Leu), 4.37 (d, ^3J(H, H) = 7.8 Hz, 0.5H, $H_{1\alpha}$), 4.20 (m, 1H, C*H*$_\alpha$–Val), 3.96 (m, 1H, H_3), 3.76–3.37 (m, 14H, H_2, H_4, H_5, H_6, O–*CH*$_2$–CH_2–*CH*$_2$–N_3, O–*CH*$_2$–CH_2CO, O*CH*$_3$), 2.48 (m, 2H, OCH_2–*CH*$_2$–CO), 2.10 (m, 1H, C*H*$_\beta$–Val), 1.85 (m, 2H, OCH_2–*CH*$_2$–*CH*$_2N_3$), 1.62–1.52 (m, 3H, *CH*$_{2\beta}$–Leu and *CH*$_\gamma$–Leu), 0.97–0.86 (m, 12H, *CH*$_3$–Val and *CH*$_3$–Leu); ^{13}C NMR (75 MHz, $CDCl_3$, 25 °C): δ = 173.1, 171.3, 170.9, 138.8, 138.5, 138.3, 138.2, 138.1, 128.4, 128.3, 128.0, 127.9, 127.9, 127.8, 127.7, 127.6, 127.5, 103.6, 97.0, 84.6, 82.2, 81.9, 80.1, 75.6, 75.6, 75.0, 74.9, 74.9, 74.6, 73.1, 67.0, 69.8, 69.4, 67.5, 67.2, 66.6, 64.8, 59.9, 58.5, 53.4, 52.2, 48.5, 48.3, 41.3, 37.0, 36.7, 30.6, 30.5, 29.2, 28.8, 24.9, 22.7, 21.9, 19.2, 18.4; IR (neat): ν = 3290 (N–H), 2097 (N_3), 1745 (C=O), 1640 (C=O); MS (ESI, ion polarity positive): *m*/*z*: 832 $[M+H]^+$, 654 $[M+Na]^+$; HRMS (TOF ESI, ion polarity positive): calcd for $C_{45}H_{61}N_5O_{10}Na$: 854.4316; found: 854.4319.

*4.1.2.8. Synthesis of compound **13**.* To a solution of **11** (1.5 g, 2.0 mmol) in DCM (8 ml) were added successively NaH (90 mg, 2.2 mmol) and trichloroacetonitrile (1.74 g, 12 mmol). The reaction mixture was stirred 3 h at rt then the solvent was removed under reduced pressure and the residue was dissolved in DCM (14 ml). Azidoethanol (209 mg, 2.4 mmol) and $BF_3{\cdot}OEt_2$ (284 mg, 2 mmol) were added and the reaction mixture was stirred 3 h at −20 °C then quenched by addition of ice. The quenched reaction was extracted by DCM and the organic layer was washed by water (3 ml), an aqueous 5% $NaHCO_3$ solution (3 ml) and brine (3 ml). The organic layer was dried over $MgSO_4$, filtered and evaporated under reduced pressure. The crude residue was purified by chromatography on a silica gel column (DCM/Et_2O, 8:2) to afford the desired product **13** as a colorless oil (810 mg, 49%, ratio α:β = 1:1). ^{1}H NMR (400 MHz, $CDCl_3$, 25 °C): δ = 7.37–7.26 (m, 15H, H_{arom}), 6.77 (m, 1H, *NH*–Val), 6.46 (m, 1H, *NH*–Leu), 5.00–4.44 (m, 7.5H, $H_{1\beta}$, 3 × Ph*CH*$_2$ and C*H*$_\alpha$–Leu), 4.43 (d, ^3J(H, H) = 7.6 Hz. 0.5H, $H_{1\alpha}$), 4.22 (m, 1H, C*H*$_\alpha$–Val), 3.96 (m, 1H, H_3), 3.81–3.41 (m, 14H, H_2, H_4, H_5, H_6, O*CH*$_2$*CH*$_2N_3$, O*CH*$_2$ and O*CH*$_3$), 2.48 (m, 2H, *CH*$_2$–CO), 2.29 (m, 1H, C*H*$_\beta$–Val), 1.65–1.51 (m, 3H, *CH*$_{2\beta}$–Leu and *CH*$_\gamma$–Leu), 0.98–0.87 (m, 12H, *CH*$_3$–Val and *CH*$_3$–Leu); ^{13}C NMR (75 MHz, $CDCl_3$, 25 °C): δ = 173.0, 171.3, 171.3, 170.9, 170.8, 138.8, 138.5, 138.4, 138.3, 138.1, 128.4, 128.3, 128.1, 128.0, 127.9, 127.8, 127.8, 127.7, 127.7, 127.6, 127.5, 127.5, 103.6, 97.2, 84.5, 82.1, 81.6, 81.6, 79.9, 75.6, 75.6, 74.9, 74.8, 74.6, 73.1, 69.8, 69.4, 68.1, 67.4, 67.1, 70.1, 58.4, 52.1, 51.0, 50.7, 50.6, 41.2, 36.9, 36.7, 30.7, 30.6, 24.8, 22.7, 21.9, 19.2, 18.4, 18.2, IR (neat): ν = 3270 (O–H), 2102 (N_3), 1745 (C=O), 1638 (C=O); MS (ESI, ion polarity positive): *m*/*z*: 818 $[M+H]^+$; HRMS (TOF ESI, ion polarity positive): calcd for $C_{44}H_{59}N_5O_{10}Na$: 840.4160; found: 840.4160.

*4.1.2.9. Synthesis of compound **14**.* A solution of **12** (470 mg, 0.56 mmol) and triphenylphosphine (297 mg, 1.1 mmol) in THF/water 9:1 (2.8 ml) was stirred for 24 h. The solvent was removed under reduced pressure and the crude residue was purified by chromatography on a silica gel column (DCM/Et_2O, 2:8 then DCM/MeOH/aqueous sol NH_4OH, 87:9:4) to afford the desired product **14** as a yellow oil (355 mg, 78%). ^{1}H NMR (300 MHz, $CDCl_3$, 25 °C): δ = 7.36–7.23 (m, 15H, H_{arom}), 6.96 (d, ^3J(H, H) = 8.4 Hz, 1H, *NH*–Val), 6.36 (d, ^3J(H, H) = 7.8 Hz, 1H, *NH*–Leu), 4.99–4.49 (massif, 7.5H, $H_{1\beta}$, 3 × Ph*CH*$_2$, C*H*$_\alpha$–Leu), 4.38 (d, ^3J(H, H) = 7.8 Hz, 0.5H, $H_{1\alpha}$), 4.15 (t, ^3J(H, H) = 8.0 Hz, 1H, C*H*$_\alpha$–Val), 3.96 (m, 1H, H_3), 3.84–3.39 (m, 14H, H_2, H_4, H_5, H_6, O–*CH*$_2$–CH_2–*CH*$_2$–N_3, O–*CH*$_2$–CH_2CO, O*CH*$_3$), 2.47 (m, 2H, OCH_2–*CH*$_2$–CO), 2.07 (m, 1H, C*H*$_\beta$–Val), 1.81 (m, 2H, OCH_2–*CH*$_2$–CH_2NH_2), 1.67–1.53 (m, 3H, *CH*$_{2\beta}$–Leu and *CH*$_\gamma$–Leu), 1.01–0.89 (m, 12H, *CH*$_3$–Val and *CH*$_3$–Leu); ^{13}C NMR (75 MHz, $CDCl_3$, 25 °C): δ = 173.2, 172.3, 171.7, 171.4, 171.3, 138.8, 138.5, 138.3, 138.2, 177.9, 128.5, 128.4, 128.1, 128.0, 127.9, 127.9, 127.8, 103.9, 97.1, 84.5, 82.1, 80.1, 77.7, 74.4, 70.1, 75.0, 75.2, 75.1, 74.9, 73.3, 70.2, 69.8, 67.7, 67.4, 67.2, 66.4, 58.9, 52.3, 51.1, 50.8, 41.3, 41.0, 39.3, 36.7, 30.5, 30.5, 24.8, 22.8, 22.0, 21.9, 19.3, 18.8, 18.4; IR (neat): ν = 3306 (N–H), 1744 (C=O), 1641 (C=O); MS (ESI, ion polarity positive): *m*/*z*: 806 $[M+H]^+$; HRMS (TOF ESI, ion polarity positive): calcd for $C_{45}H_{64}N_3O_{10}$: 806.4592; found: 806.4590.

*4.1.2.10. Synthesis of compound **15**.* Same procedure as described for **14** from compound **13** (711 mg, 0.87 mmol) to afford the desired product **15** as a pale yellow oil (688 mg, 76%). ^{1}H NMR (300 MHz, $CDCl_3$, 25 °C): δ = 7.72 (m, 1H, NH), 7.33–7.25 (m, 15H, H_{arom}), 6.94 (d, ^3J(H, H) = 8.4 Hz, 1H, NH), 6.80 (m, 1H, NH), 6.55 (d, ^3J(H, H) = 7.8 Hz, 1H, NH), 5.00–4.51 (m, 7.5H, $H_{1\beta}$, 3 × Ph*CH*$_2$ and C*H*$_\alpha$–Leu), 4.34 (d, ^3J(H, H) = 7.8 Hz, 0.5H, $H_{1\alpha}$), 4.18 (m, 1H, C*H*$_\alpha$-Val), 3.97 (m, 1H, H_3), 3.80–2.89 (massif, 16H, NH_2, H_2, H_4, H_5, H_6, O*CH*$_2$*CH*$_2$$NH_2$, O*CH*$_2$ and O*CH*$_3$), 2.48 (m, 2H, *CH*$_2$–CO), 2.09 (m, 1H, C*H*$_\beta$–Val), 1.65–1.52 (m, 3H, *CH*$_{2\beta}$–Leu and *CH*$_\gamma$–Leu), 1.03–0.87 (m, 12H, *CH*$_3$–Val and *CH*$_3$–Leu); ^{13}C NMR (75 MHz, $CDCl_3$, 25 °C): δ = 173.1, 171.7, 171.3, 171.1, 138.7, 138.3, 138.2, 138.1, 128.4, 128.4, 128.3, 128.0, 127.9, 127.9, 127.6, 104.5, 97.2, 84.5, 82.0, 81.9, 80.0, 74.3, 75.6, 75.0, 75.0, 74.3, 73.2, 70.6, 70.0, 69.7, 67.8, 67.3, 59.7, 58.7, 52.2, 51.0, 50.7, 41.5, 41.2, 36.8, 36.3, 30.3, 30.3, 24.8, 22.8, 21.9, 19.2, 18.9, 18.3; IR (neat): ν = 3262 (N–H), 3206 (N–H), 3178 (N–H), 1745 (C=O), 1641 (C=O); $C_{42}H_{56}N_2O_{10}$ + 3.6H_2O: calcd C 61.68, H 8.02, N 4.90; found C 61.72, H 7.76, N 4.77; MS (ESI, ion polarity positive): *m*/*z*: 792 $[M+H]^+$; HRMS (TOF ESI, ion polarity positive): calcd for $C_{44}H_{62}N_3O_{10}$: 792.4435; found: 792.4456.

*4.1.3. Synthesis of compounds **16** and **17***

To a solution of N-Boc–L-Val (172 mg, 0.79 mmol) in DMF (15 ml) were added HBTU (300 mg, 0.79 mmol), HOBt (107 mg, 0.79 mmol), DIPEA (0.21 ml, 1.2 mmol) and **14** (319 mg, 0.4 mmol). The reaction mixture was stirred for 40 h at rt then the solvent was removed under reduced pressure and the residue was dissolved in EtOAc (25 ml). This solution was washed with water (25 ml), an aqueous 10% citric acid solution (25 ml), an aqueous saturated $NaHCO_3$ solution (25 ml) and brine (25 ml). The organic layer was dried over $MgSO_4$, filtered and evaporated under reduced pressure. The crude residue was purified by chromatography on a silica gel column (cyclohexane/AcOEt, 35:65 then 20:80) to afford **16** as a white solid (222 mg, 56%) and **17** as a pale yellow solid (138 mg, 35%).

*4.1.3.1. Compound **16**.* ^{1}H NMR (300 MHz, $CDCl_3$, 25 °C): δ = 7.26–7.22 (m, 15H, H_{arom}), 7.09 (br s, 1H, $OCH_2CH_2CH_2$–*NH*), 6.77 (d, ^3J(H, H) = 6.5 Hz, 1H, *NH*–Leu), 6.64 (d, ^3J(H, H) = 7.7 Hz, 1H, *NH*–Val), 5.24 (br s, 1H, *NH*–Boc), 4.90–4.50 (m, 7H, 3 × Ph*CH*$_2$, C*H*$_\alpha$–Leu), 4.33 (d, ^3J(H, H) = 7.9 Hz 1H, $H_{1\alpha}$), 4.25 (m, 1H, C*H*$_\alpha$–Val), 4.02 (m, 1H, C*H*$_\alpha$–BocVal), 3.88 (m, 1H, O–C*H*H–CH_2–CH_2–NH), 3.72–3.58 (m, 9H, H_3, H_6, O–C*H*H–CH_2–*CH*H–NH, O–C*H*H–CH_2CO, O*CH*$_3$), 3.48–3.33 (m, 4H, H_2, H_4, H_5, O–CH_2–CH_2–*CH*H–NH), 3.18 (m, 1H, O–C*H*H–CH_2CO), 2.37 (m, 2H, OCH_2–*CH*$_2$–CO), 2.08–1.78 (m, 4H, OCH_2–*CH*$_2$–CH_2NH, 2 × C*H*$_\beta$–Val), 1.61–1.49 (m, 3H, *CH*$_{2\beta}$–Leu and *CH*$_\gamma$–Leu), 1.39 (s, 9H, CH_3–Boc), 0.95–0.85 (m, 18H,

2 × *CH*$_3$–Val and *CH*$_3$–Leu); ^{13}C NMR (75 MHz, $CDCl_3$, 25 °C): δ = 173.0, 171.4, 138.6, 138.4, 138.1, 128.4, 128.4, 128.0, 127.8, 127.7, 127.6, 103.8, 84.6, 82.2, 81.0, 77.6, 75.6, 75.0, 74.8, 69.7, 67.7, 67.7, 59.2, 58.4, 52.1, 50.9, 40.8, 36.8, 36.4, 31.7, 30.9, 29.7, 28.4, 24.8, 22.8, 21.8, 19.1, 18.7; m.p. 140–142 °C; IR (neat): ν = 3310 (N–H), 2961 (N–H), 1637 (C=O); MS (ESI, ion polarity positive): *m*/*z*: 1006 $[M+H]^+$; HRMS (TOF ESI, ion polarity positive): calcd for $C_{55}H_{80}N_4O_{13}Na$: 1027.5620; found: 1027.5619.

4.1.3.2. Compound ***17***. ^{1}H NMR (300 MHz, $CDCl_3$, 25 °C): δ = 7.37–7.26 (m, 15H, H_{arom}), 6.82–6.79 (br s, 2H, $OCH_2CH_2CH_2$–*NH* and *NH*–Leu), 6.45 (br s, 1H, *NH*–Val), 5.20 (br s, 1H, *NH*–Boc), 5.03–4.50 (m, 8H, $H_{1\beta}$, 3 × Ph*CH*$_2$, C*H*$_\alpha$–Leu), 4.22 (m, 1H, C*H*$_\alpha$–BocAla), 4.07–3.96 (m, 2H, H_3, C*H*$_\alpha$–Val), 3.75–3.62 (m, 8H, H_5, H_6, O–C*H*H–CH_2–CH_2–NH, O–*CH*$_2$–CH_2CO, O*CH*$_3$), 3.54–3.39 (m, 5H, H_2, H_4, H_6, O–C*H*H–CH_2–*CH*H–NH), 3.25 (m, 1H, O–CH_2–CH_2–C*H*H–NH), 2.47 (m, 2H, OCH_2–*CH*$_2$–CO), 2.07–1.82 (m, 4H, OCH_2–*CH*$_2$–CH_2NH, 2 × C*H*$_\beta$–Val), 1.64–1.51 (m, 3H, *CH*$_{2\beta}$–Leu and *CH*$_\gamma$–Leu), 1.42 (s, 9H, CH_3–Boc), 0.95–0.85 (m, 18H, 2 × *CH*$_3$–Val and *CH*$_3$–Leu); ^{13}C NMR (75 MHz, $CDCl_3$, 25 °C): δ = 171.3, 171.2, 139.0, 138.1, 128.5, 128.4, 128.4, 128.1, 128.0, 127.8, 127.5, 97.4, 84.6, 82.1, 81.0, 77.9, 75.7, 75.0, 70.0, 67.2, 59.2, 58.4, 52.2, 50.9, 41.1, 37.5, 36.7, 31.7, 30.9, 29.7, 28.4, 24.8, 22.8, 21.9, 19.4, 19.2, 18.4; m.p. 144–146 °C; IR (neat): ν = 3304 (N–H), 2952 (N–H), 1645 (C=O); MS (ESI, ion polarity positive): *m*/*z*: 1006 $[M+H]^+$; HRMS (TOF, ion polarity positive): calcd for $C_{55}H_{80}N_4O_{13}Na$: 1027.5620; found: 1027.5627.

4.1.4. Synthesis of compounds ***18*** *and* ***19***

Same procedure as described for **16** and **17** from compound **15** (457 mg, 0.58 mmol) to afford **18** as a white solid (256 mg, 45%) and **19** as a yellowish solid (226 mg, 40%).

4.1.4.1. Compound ***18***. ^{1}H NMR (300 MHz, $CDCl_3$, 25 °C): δ = 7.30–7.25 (m, 15H, H_{arom}), 7.17 (br s, 1H, OCH_2CH_2–*NH*), 7.06 (br s, 1H, *NH*–Val), 6.80 (br s, 1H, *NH*–Leu), 5.29 (br s, 1H, *NH*–Boc), 4.94–4.53 (m, 7H, and 3 × Ph*CH*$_2$, C*H*$_\alpha$–Leu), 4.38 (t, ^3J(H, H) = 7.8 Hz, 1H, $H_{1\alpha}$), 4.25 (m, 1H, C*H*$_\alpha$–Val), 3.97 (m, 1H, C*H*$_\alpha$–BocVal), 3.82–3.36 (m, 15H, H_2, H_3, H_4, H_5, H_6, O*CH*$_2$*CH*$_2$NH, O–*CH*$_2$–CH_2CO, O*CH*$_3$), 2.55 (m, 2H, OCH_2–*CH*$_2$–CO), 2.13–1.99 (m, 2H, 2 × C*H*$_\beta$–Val), 1.66–1.56 (m, 3H, *CH*$_{2\beta}$–Leu and *CH*$_\gamma$–Leu), 1.43 (s, 9H, *CH*$_3$–Boc), 0.99–0.87 (m, 18H, 2 × *CH*$_3$–Val and *CH*$_3$–Leu); ^{13}C NMR (75 MHz, $CDCl_3$, 25 °C): δ = 172.9, 171.8, 171.2, 171.3, 155.9, 138.5, 138.3, 138.0, 128.4, 128.4, 128.0, 127.8, 127.7, 127.6, 103.8, 84.5, 82.2, 77.5, 75.6, 75.0, 74.0, 74.6, 69.8, 67.7, 67.4, 59.9, 58.9, 52.2, 51.0, 40.8, 40.0, 36.5, 36.4, 31.6, 30.5, 28.3, 24.8, 22.7, 21.8, 19.2, 19.1, 18.7, 17.8; m.p. 144–146 °C; $C_{54}H_{78}N_4O_{13}$ + 6.0H_2O: calcd C 59.0, H 8.25, N 5.10; found C 58.78, H 7.29, N 4.95; IR (neat): ν = 3283 (N–H), 2957 (N–H), 1636 (C=O); MS (ESI, ion polarity positive): *m*/*z*: 992 $[M+H]^+$; HRMS (TOF ESI, ion polarity positive): calcd for $C_{54}H_{78}N_4O_{13}Na$: 1013.5463; found: 1013.5443.

4.1.4.2. Compound ***19***. ^{1}H NMR (400 MHz, $CDCl_3$, 25 °C): δ = 7.33–7.25 (m, 15H, H_{arom}), 6.92 (br s, 1H, OCH_2CH_2–*NH*), 6.77 (br s, 1H, *NH*–Val), 6.47 (br s, 1H, *NH*–Leu), 5.10 (sl, 1H, *NH*–Boc), 4.99–4.51 (m, 8H, $H_{1\beta}$, 3 × Ph*CH*$_2$ and C*H*$_\alpha$–Leu), 4.21 (m, 1H, C*H*$_\alpha$–Val), 3.98–3.93 (m, 2H, H_3, C*H*$_\alpha$–BocVal), 3.78 (m, 1H, H_5), 3.70–3.65 (m, 7H, H_2, H_6, O–*CH*$_2$–CH_2NH, O*CH*$_3$), 3.57–3.48 (m, 5H, H_6, OCH_2–*CH*$_2$–NH, O–*CH*$_2$–CH_2CO), 3.37 (t, *J* = 9.6 Hz, 1H, H_4), 2.47 (m, 2H, OCH_2–*CH*$_2$–CO), 2.13–1.99 (m, 2H, 2 × C*H*$_\beta$–Val), 1.65–1.51 (m, 3H, *CH*$_{2\beta}$–Leu and *CH*$_\gamma$–Leu), 1.42 (s, 9H, *CH*$_3$–Boc), 0.98–0.85 (m, 18H, 2 × *CH*$_3$–Val and *CH*$_3$–Leu); ^{13}C NMR (100 MHz, $CDCl_3$, 25 °C): δ = 173.0, 171.8, 172.2, 171.1, 155.9, 138.7, 138.1, 138.0, 128.5, 128.4, 128.0, 127.9, 127.8, 127.7, 127.6, 97.1, 82.0, 79.9, 78.0, 75.6, 75.0, 73.3, 70.3, 70.1, 70.1, 67.1, 59.7, 58.7, 52.2, 50.8, 41.1, 39.0, 36.7, 36.6, 31.3, 30.5, 28.3, 24.8, 22.7, 21.9, 19.3, 19.1, 18.4, 17.8; m.p. 160–162 °C; $C_{54}H_{78}N_4O_{13}$: calcd C 65.43, H 7.93, N 5.65; found C 65.41, H 7.94, N 5.55; IR (neat): ν = 3281 (N–H), 2955 (N–H), 1640 (C=O); MS (ESI, ion polarity positive, MeOH): *m*/*z*: 992 $[M+H]^+$; HRMS (TOF, ion polarity positive): calcd for $C_{54}H_{78}N_4O_{13}Na$: 1013.5463; found: 1013.5447.

4.1.5. Synthesis of protected peptidomimetics ***20***–***23***

4.1.5.1. Compound ***20***. A solution of **16** (124 mg, 0.123 mmol) in DCM/TFA 1:1 (0.6 ml) was stirred for 2 h at rt then the solvent was removed under reduced pressure and the residue was dissolved in DMF (1.5 ml). To the resulting solution were added *N*-Boc–L-alanine (47 mg, 0.25 mmol), HBTU (94 mg, 0.25 mmol), HOBt (33 mg, 0.25 mmol) and DIPEA (0.09 ml, 0.50 mmol). The reaction mixture was stirred for 48 h at rt then the solvent was removed under reduced pressure and the residue was dissolved in EtOAc (8 ml). This solution was washed with water (8 ml), an aqueous 10% citric acid solution (8 ml), an aqueous saturated $NaHCO_3$ solution (8 ml) and brine (8 ml). The organic layer was dried over $MgSO_4$, filtered and evaporated under reduced pressure. The crude residue was purified by chromatography on a silica gel column (DCM/MeOH, 98:2) to afford **20** as a white solid (91 mg, 68%). ^{1}H NMR (300 MHz, $CDCl_3$, 25 °C): δ = 7.64–7.41 (br s, 1H, NH), 7.37–7.26 (m, 15H, H_{arom}), 6.87–6.76 (br s, 2H, NH), 5.26 (br s, 1H, *NH*-Boc), 4.93–4.16 (m, 11H, $H_{1\alpha}$, H_3, 3 × Ph*CH*$_2$, C*H*$_\alpha$–Leu4, C*H*$_\alpha$–Val3, C*H*$_\alpha$–Ala1), 3.87–3.13 (m, 15H, H_2, H_4, H_5, H_6, C*H*$_\alpha$–Val2, O–*CH*$_2$–CH_2–*CH*$_2$–NH, O*CH*$_2$–CH_2–CO, O*CH*$_3$), 2.37 (m, 2H, OCH_2–*CH*$_2$–CO), 2.10–1.82 (m, 4H, OCH_2–*CH*$_2$–CH_2NH, 2 × C*H*$_\beta$–Val), 1.66–1.51 (m, 3H, *CH*$_{2\beta}$–Leu and *CH*$_\gamma$–Leu), 1.43 (s, 9H, CH_3–Boc), 1.33 (d, ^3J(H, H) = 6.9 Hz, 3H, *CH*$_3$–Ala), 0.97–0.89 (m, 18H, 2 × *CH*$_3$–Val and *CH*$_3$–Leu); ^{13}C NMR (75 MHz, $CDCl_3$, 25 °C): δ = 173.9, 173.1, 171.7, 171.7, 171.3, 155.8, 138.5, 138.4, 138.0, 128.5, 128.4, 128.1, 127.9, 127.8, 127.6, 104.2, 84.5, 80.3, 77.3, 75.6, 75.1, 74.9, 74.8, 58.5, 69.4, 67.9, 67.7, 59.1, 58.5, 52.3, 50.9, 40.8, 35.9, 30.9, 30.1, 28.3, 24.8, 22.8, 21.8, 19.3, 19.1, 18.0, 18.8; m.p. decomposition; IR (neat): ν = 3281 (N–H), 2963 (N–H), 1637 (C=O); MS (ESI, ion polarity positive): *m*/*z*: 1076 $[M+H]^+$; HRMS (TOF ESI, ion polarity positive): calcd for $C_{58}H_{85}N_5O_{14}Na$: 1098.5991; found: 1098.5964.

4.1.5.2. Compound ***21***. Same procedure as described for **20** from compound **17** (197 mg, 0.196 mmol) to afford **21** as a pale yellow solid (172 mg, 88%). ^{1}H NMR (300 MHz, $CDCl_3$, 25 °C): δ = 7.34–7.25 (massif, 15H, H_{arom}), 7.02 (br s, 1H, $OCH_2CH_2CH_2$–*NH*), 6.88–6.80 (m, 3H, *NH*–Leu, *NH*–Ala, *NH*–Val), 5.14 (br s, 1H, NH–Boc), 5.02–4,53 (m, 8H, $H_{1\beta}$, H_3, 3 × Ph*CH*$_2$), 4.32–4.26 (m, 2H, C*H*$_\alpha$–Leu4, C*H*$_\alpha$–Val3), 4.16 (m, 1H, C*H*$_\alpha$–Ala1), 3.96 (t, ^3J(H, H) = 9.3 Hz, 1H, C*H*$_\alpha$–Val2), 3.78–3.64 (m, 8H, H_2, O–*CH*$_2$–CH_2–CH_2–NH, O–*CH*$_2$–CH_2CO, O*CH*$_3$), 3.54–3.23 (m, 6H, H_4, H_5, H_6, O–CH_2–CH_2–*CH*$_2$–NH), 2.37 (t, ^3J(H, H) = 5.4 Hz, 2H, OCH_2–*CH*$_2$–CO), 2.08 (m, 2H, OCH_2–*CH*$_2$–CH_2NH), 1.86–1.82 (m, 2H, 2 × C*H*$_\beta$–Val), 1.66–1.53 (m, 3H, *CH*$_{2\beta}$–Leu and *CH*$_\gamma$–Leu), 1.43 (s, 9H, CH_3–Boc), 1.33 (d, ^3J(H, H) = 6.9 Hz, 3H, *CH*$_3$–Ala), 0.94–0.86 (m, 18H, 2 × *CH*$_3$–Val and *CH*$_3$–Leu); ^{13}C NMR (75 MHz, $CDCl_3$, 25 °C): δ = 173.1, 172.7, 171.3, 170.0, 166.0, 155.0, 138.9, 138.2, 128.5, 128.5, 128.4, 128.1, 128.0, 127.9, 127.6, 97.4, 82.1, 80.0, 78.1, 75.8, 75.1, 73.4, 71.2, 70.0, 67.3, 67.3, 58.5, 58.4, 52.2, 57.4, 57.1, 41.2, 37.2, 36.9, 31.0, 30.9, 29.5, 28.3, 24.2, 22.8, 22.0, 19.4, 19.2, 17.8, 18.4; m.p. decomposition; IR (neat): ν = 3294 (N–H), 2968 (N–H), 1636 (C=O); MS (ESI, ion polarity positive): *m*/*z*: 1076 $[M+H]^+$; HRMS (TOF ESI, ion polarity positive): calcd for $C_{58}H_{85}N_5O_{14}Na$: 1098.5991; found: 1098.5939.

4.1.5.3. Compound ***22***. Same procedure as described for **20** from compound **18** (135 mg, 0.136 mmol) to afford **22** as a white solid (138 mg, 76%). ^{1}H NMR (400 MHz, $CDCl_3$, 25 °C): δ = 7.36–7.25 (m,

16H, H_{arom}, NH), 7.14 (d, ^3J(H, H) = 9.0 Hz, 1H, NH), 6.90 (d, ^3J(H, H) = 7.2 Hz, 1H, NH), 6.78 (d, ^3J(H, H) = 9.3 Hz, 1H, NH), 5.36 (br s, 1H, NH–Boc), 4.95–4.55 (m, 7H, $H_{1\alpha}$, 3 × PhCH_2), 4.38–4.26 (m, 3H, CH_α–Leu, CH_α–Val4, H_3), 4.17 (m, 1H, CH_α–Val2), 3.96 (m, 1H, CH_α–Ala1), 3.84–3.25 (m, 14H, H_2, H_4, H_5, H_6, OCH_2CH_2NH, O–CH_2–CH_2CO, OCH_3), 2.59 (m, 2H, OCH$_2$–CH_2–CO), 2.14–1.96 (m, 2H, 2 × CH_β–Val), 1.68–1.51 (m, 3H, $CH_{2\beta}$–Leu and CH_γ–Leu), 1.43 (s, 9H, CH_3–Boc), 1.33 (d, ^3J(H, H) = 6.9 Hz, 3H, CH_3–Ala1), 0.98–0.90 (m, 18H, 2 × CH_3–Val and CH_3–Leu); ^{13}C NMR (100 MHz, $CDCl_3$, 25 °C): δ = 172.7, 171.2, 170.9, 138.5, 138.3, 137.9, 128.5, 128.4, 128.1, 128.1, 127.9, 127.8, 127.6, 104.1, 84.5, 82.2, 77.6, 75.6, 75.1, 74.9, 74.7, 70.0, 67.8, 58.5, 58.2, 52.1, 50.8, 41.1, 40.3, 36.8, 31.8, 30.9, 28.3, 24.8, 22.7, 22.0, 19.3, 19.2, 18.5, 18.1; m.p. decomposition; IR (neat): ν = 3273 (N–H), 2964 (N–H), 1638 (C=O); MS (ESI, ion polarity positive): m/z: 1063 $[M+H]^+$; HRMS (TOF ESI, ion polarity positive): calcd for $C_{57}H_{83}N_5O_{14}Na$: 1084.5834; found: 1084.5862.

*4.1.5.4. Compound **23**.* Same procedure as described for **20** from compound **19** (177 mg, 0.18 mmol) to afford **23** as a pale yellow solid (142 mg, 75%). ^{1}H NMR (400 MHz, $CDCl_3$, 25 °C): δ = 7.33–7.24 (m, 15H, H_{arom}), 7.17 (m, 1H, NH), 6.95 (d, ^3J(H, H) = 8.7 Hz, 1H, NH), 6.87 (d, ^3J(H, H) = 8.1 Hz, 1H, NH), 6.81 (d, ^3J(H, H) = 8.7 Hz, 1H, NH), 4.87–4.53 (m, 8H, $H_{1\beta}$, H_3, 3 × PhCH_2), 4.33 (t, ^3J(H, H) = 8.1 Hz, 1H, CH_α–Leu), 4.24 (t, ^3J(H, H) = 7.2 Hz, 1H, CH_α–Val4), 4.16 (m, 1H, CH_α–Val2), 3.97–3.25 (m, 15H, H_2, H_4, H_5, H_6, OCH_2CH_2NH, CH_α–Ala1, O–CH_2–CH_2CO, OCH_3), 2.52 (m, 2H, OCH$_2$–CH_2–CO), 2.09–2.01 (m, 2H, 2 × CH_β–Val), 1.66–1.54 (m, 3H, $CH_{2\beta}$–Leu and CH_γ–Leu), 1.43 (s, 9H, CH_3–Boc), 1,31 (d, ^3J(H, H) = 7.2 Hz, 3H, CH_3–Ala1), 0.94–0.89 (m, 18H, 2 × CH_3–Val and CH_3–Leu); ^{13}C NMR (100 MHz, $CDCl_3$, 25 °C): δ = 173.1, 172.8, 171.2, 171.0, 138.1, 128.5, 128.4, 128.0, 127.9, 127.8, 127.6, 97.3, 82.0, 79.9, 78.1, 75.7, 74.9, 73.4, 70.5, 70.4, 67.6, 67.2, 58.5, 58.4, 52.1, 50.8, 41.2, 39.3, 36.8, 31.3, 31.0, 28.3, 24.8, 22.7, 22.0, 19.3, 19.2, 18.4; m.p. decomposition; IR (neat): ν = 3275 (N–H), 2957 (N–H), 1639 (C=O); MS (ESI, ion polarity positive): m/z: 1063 $[M+H]^+$; HRMS (TOF ESI, ion polarity positive): calcd for $C_{57}H_{83}N_5O_{14}Na$: 1084.5834; found: 1084.5801.

4.2. Amyloid peptide preparation

The syntheses of $A\beta_{1-40}$ and IAPP were performed at the Institut de Biologie Intégrative (IFR83) at the University Pierre et Marie Curie. $A\beta_{1-40}$ and IAPP with an amidated C-terminus were synthesized using Fmoc chemistry. The peptides were then purified by HPLC and characterized by MALDI-TOF mass spectrometry. IAPP and $A\beta_{1-40}$ were dissolved in hexafluoro-isopropanol (HFIP) at a concentration of 1 mM and 0.5 mM respectively, and incubated for at least 1 h to dissolve any preformed aggregates. Next, HFIP was evaporated with dry nitrogen gas followed by vacuum desiccation for at least 1 h. The resulting peptide film was then dissolved in DMSO for the microscopy and ThT experiments to obtain stock solutions of IAPP (0.2 mM) and $A\beta_{1-40}$ (0.4 mM). For those experiments, we used the same concentration of DMSO (2.5% in the final volume) and hence we were able to compare for those experiments the shape of the curve and the lag time.

4.3. Thioflavin-T assay

Thioflavin-T binding assays were used to measure the development of fibrils over time. A plate reader (Fluostar Optima, BmgLabtech) and standard 96-wells flat-bottom black microtiter plates in combination with a 440 nm excitation filter and a 485 nm emission filter were used. For the IAPP/peptidomimetics experiments, the ThT assay was started by adding 5 μL of a 0.2 mM IAPP stock solution and between 0.5 and 50 μL of a 0.2 mM peptidomimetics stock solution to a mixture of 10 μM ThT and 10 mM Tris/HCl, 100 mM NaCl at pH 7.4. The concentration of IAPP was held constant at 5 μM and the peptidomimetics were added in equimolar amounts to yield 1:10 and 1:1 molar ratio mixtures. For $A\beta_{1-40}$, the ThT was measured on aliquots of $A\beta_{1-40}$ incubations (20 μM) made in 10 mM Tris/HCl, 100 mM NaCl at pH 7.4. For the studies on the effects of the peptidomimetics on $A\beta_{1-40}$ fibrillogenesis at different time points, stock solutions of peptidomimetics were mixed with a stock solution of $A\beta_{1-40}$ at different $A\beta_{1-40}$:peptidomimetics ratios (1:1 and 1:0.1) in a mixture of 10 μM ThT and 10 mM Tris/HCl, 100 mM NaCl at pH 7.4. The ThT assays were performed between 2 and 6 times, on different days, using different IAPP and $A\beta_{1-40}$ stock solutions.

The assessment of inhibition of amyloid peptide aggregation by peptidomimetic was determined as followed. Amyloid peptide aggregation assays were performed in the absence and presence of peptidomimetic and fibril formation was monitored via ThT fluorescence to evaluate each compound's ability to alter both the lag time to aggregate formation and the equilibrium plateau indicative of the quantity of aggregate formed. The extension of the lag time was evidenced as an increase in the experimental lag time in the presence of the peptidomimetic relative to the lag time observed without the peptidomimetic, and is evaluated as a ratio, $t_{A\beta\,+\,peptidomimetic}/t_{A\beta}$. The reduction of the equilibrium plateau was evidenced as a decrease in the experimental fluorescence plateau with the peptidomimetic, relative to the fluorescence plateau observed without the peptidomimetic, and is evaluated as the percentage decrease from the experimental fluorescence plateau with the peptidomimetic, $(F_{A\beta} - F_{A\beta\,+\,peptidomimetic})/F_{A\beta} \times 100\%$.

4.4. Transmission electron microscopy

TEM was performed at the Institut de Biologie Intégrative (IFR83) at the University Pierre et Marie Curie. Peptides were incubated under the same conditions as in the ThT assay. Aliquots (20 μL) of this mixture were adsorbed onto carbon-coated 300-mesh copper grids for 2 min. The grids were then blotted and dried. Next, the grids were negatively stained for 45 s on 2.5% uranyl acetate in 1:1 ethanol/water, and again blotted and dried. The grids were examined using a ZEISS 912 Omega electron microscope operating at 80 kV.

4.5. NMR studies

NMR experiments on peptidomimetics **1**–**4** were recorded on a Bruker AVANCE III 500 MHz spectrometer equipped with a TCI triple resonance cryogenic probe with *Z*-axis gradient. Experiments were processed with Bruker TOPSPIN 2.0 software. ^{1}H and ^{13}C resonances were assigned in $CDCl_3$, using 2D COSY, 2D TOCSY (70 ms mixing time), 2D ROESY (300 ms mixing time), 2D ^{1}H–^{13}C HSQC and 2D ^{1}H–^{13}C HMBC spectra. 1D spectra were acquired over 32 K data points using a spectral width of 5000 Hz. Typically, 512 increments were acquired over a spectral width of 5000 Hz. Prior to Fourier Transformation in t_2 and t_1 dimensions, time domain data were zero-filled and multiplied by a $\pi/3$-shifted square sinebell function. The ^{1}H and ^{13}C resonance assignments are listed in Tables S1–S4 (Supplementary data). The temperature gradients of the amide proton chemical shifts were derived from 1D and 2D TOCSY spectra recorded at 279.5, 284.5, 294.5, 299.5 K. ^3J coupling constants were measured on 1D spectra at 284.5 K.

*4.5.1. Conformation studies of peptidomimetics **1**–**4***

The conformation of peptidomimetics **1**–**4** was studied in aqueous solution, either in H_2O/D_2O (90:10 v/v) or in 50 mM sodium phosphate, 150 mM NaCl, pH 7.0 containing 10% D_2O. The ^{1}H resonance assignments are listed in Tables S5–S8. TOCSY

experiments were recorded with a mixing time of 70 ms. ROESY spectra were acquired with a mixing time of 300 ms. The solvent signal was suppressed using a WATERGATE sequence.

*4.5.2. Interaction studies of peptidomimetic **1** with $A\beta_{1-40}$*

The interaction of peptidomimetic **1** with $A\beta_{1-40}$ was studied in an aqueous solution of 50 mM sodium phosphate, 150 mM NaCl, pH 7.0 containing 10% D_2O. 2D NOESY experiments were recorded with a mixing time of 0.2 s. 1D STD experiments were recorded using a cascade of Gaussian shaped selective pulses (50 ms duration, B_1 field of 0.16 kHz) for a total duration of 2 s, applied at −1 and +30 ppm alternatively.

Acknowledgements

We thank Claire Troufflard and Amaury Griffon du Bellay for NMR experiments and help with sugar amino acid derivatives synthesis, respectively. We thank the Ministère de l'Enseignement Supérieur et de la Recherche (MESR) for financial support of BD. Christophe Piesse and Géraldine Toutirais (IFR83-Université Pierre et Marie Curie, France) are acknowledged for the amyloid peptides syntheses and the electron microscopy, respectively.

Appendix. Supplementary data

Supplementary data associated with this article can be found in the online version, at doi:10.1016/j.ejmech.2011.10.008.

References

[1] (a) K. Blennow, M.J. de Leon, H. Zetterberg, Lancet 368 (2006) 387–403; (b) A. Abbott, Nature 475 (2011) S2–S4.
[2] M. Goedert, M.G. Spillantini, Science 314 (2006) 777–781.
[3] H. Mori, K. Takio, M. Ogawara, D.J. Selkoe, J. Biol. Chem. 267 (1992) 17082–17086.
[4] S. Vivekanandan, J.R. Brender, S.Y. Lee, A. Ramamoorthy, Biochem. Biophys. Res. Commun. 411 (2011) 312–316.
[5] (a) A.T. Petkova, W.M. Yau, R. Tycko, Biochemistry 45 (2006) 498–512; (b) L. Yu, R. Edalji, J.E. Harlan, T.F. Holzman, A. Pereda Lopez, B. Labkovsky, H. Hillen, S. Barghorn, U. Ebert, P.L. Richardson, L. Miesbauer, L. Solomon, D. Bartley, K. Walter, R.W. Johnson, P.J. Hajduk, E.T. Olejniczak, Biochemistry 48 (2009) 1870–1877.
[6] R. Roychaudhuri, M. Yang, M.M. Hoshi, D.B. Teplow, J. Biol. Chem. 284 (2009) 4749–4753.
[7] D.J. Selkoe, Behav. Brain. Res. 192 (2008) 106–113.
[8] K.N. Dahlgren, A.M. Manelli, W.B. Stine, L.K. Baker, G.A. Krafft, M.J. LaDu, J. Biol. Chem. 277 (2002) 32046–32053.
[9] K. Ono, M.M. Condron, D.B. Teplow, Proc. Natl. Acad. Sci. U.S.A. 106 (2009) 14745–14750.
[10] (a) A. Jan, O. Adolfsson, I. Allaman, A.-L. Buccarello, P.J. Magistretti, A. Pfeifer, A. Muhs, H.A. Lashuel, J. Biol. Chem. 286 (2011) 8585–8596; (b) M.F.M. Engel, L. Khemtémourian, C.C. Kleijer, H.J.D. Meeldijk, J. Jacobs, A.J. Verkeij, B. de Kruijff, J.A. Killian, J.W.M. Höppener, Proc. Natl. Acad. Sci. U.S.A. 104 (2008) 6033–6038.
[11] A. Reza, A. Ladiwala, J.S. Dordick, P.M. Tessier, J. Biol. Chem. 286 (2011) 3209–3218.
[12] C. Nerelius, A. Sandegren, H. Sargsyan, R. Raunak, H. Leijonmarck, U. Chatterjee, A. Fisahn, S. Imarisio, D.A. Lomas, D.C. Crowther, R. Strömberg, J. Johansson, Proc. Natl. Acad. Sci. U.S.A. 106 (2009) 9191–9196.
[13] For a review, see C.I. Stains, K. Mondal, I. Ghosh, ChemMedChem 2 (2007) 1674–1692.
[14] W.P. Esler, E.R. Stimson, J.R. Ghilardi, Y.A. Lu, A.M. Felix, H.V. Vinters, P.W. Mantyh, J.P. Lee, J.E. Maggio, Biochemistry 35 (1996) 13914–13921.
[15] L.O. Tjenberg, J. Näslund, F. Lindqvist, A.R. Karlström, J. Thyberg, L. Terenius, C. Nordstedt, J. Biol. Chem. 271 (1996) 8545–8548.
[16] T. Takahashi, H. Mihara, Acc. Chem. Res. 41 (2008) 1309–1318.
[17] D.J. Gordon, K.L. Sciarretta, S.C. Meredith, Biochemistry 40 (2001) 8237–8245.
[18] C. Soto, E.M. Sigurdsson, L. Morelli, R.A. Kumar, E.M. Castano, B. Frangione, Nat. Med. 4 (1998) 822–826.
[19] A. Frydman-Marom, M. Rechter, I. Shefler, Y. Bram, D.E. Shalev, E. Gazit, Angew. Chem., Int. Ed. 48 (2009) 1981–1986.
[20] (a) S.A.W. Gruner, V. Truffault, G. Voll, E. Locardi, M. Stöckle, H. Kessler, Chem.—Eur. J. 8 (2002) 4366–4376; (b) F. Schweizer, Angew. Chem., Int. Ed. 41 (2002) 230–253; (c) M.D.P. Risseueuw, M. Overhand, G.W.J. Fleet, M.I. Simone, Tetrahedron: Asymmetry 18 (2007) 2001–2010.
[21] R.F. Hirschmann, K.C. Nicolaou, A.R. Angeles, J.S. Chen, A.B. Smith 3rd, Acc. Chem. Res. 42 (2009) 1511–1520.
[22] Y. Miura, K. Yasuda, K. Yamamoto, M. Koike, Y. Nishida, K. Kobayashi, Biomacromolecules 8 (2007) 2129–2134.
[23] (a) T. Ariga, T. Miyatake, R.K. Yu, J. Neurosci. Res. 88 (2010) 2303–2315; (b) J.J. Valle-Delgado, M. Alfonso-Prieto, N.S. de Groot, S. Ventura, J. Samitier, C. Rovira, X. Fernandez-Busquets, FASEB J. 24 (2010) 4250–4261.
[24] C. Rivière, J.C. Delaunay, F. Immel, C. Cullin, J.P. Monti, Neurochem. Res. 34 (2009) 1120–1128.
[25] C. Jaramillo, J.-L. Chiara, M. Martin-Lomas, J. Org. Chem. 59 (1994) 3135–3145.
[26] P. Sahai, M. Chawla, R.A. Vishwakarma, J. Chem. Soc., Perkin Trans. 1 (2000) 1283–1290.
[27] A. Dupraz, P. Guy, C. Dupuy, Tetrahedron Lett. 37 (1996) 1237–1240.
[28] H. Bazin, A. Bouchu, G. Descotes, J. Carbohydr. Chem. 14 (1995) 1187–1207.
[29] K. Jansson, G. Noori, G. Magnusson, J. Org. Chem. 55 (1990) 3181–3185.
[30] H. Rathore, T. Hashimoto, K. Igarashi, H. Nukaya, S.D. Fullerton, Tetrahedron 41 (1985) 5427–5438.
[31] P.C. Conrad, P.L. Kwiatkowski, P.L. Fuchs, J. Org. Chem. 52 (1987) 586–591.
[32] M. Dowlut, D.G. Hall, O. Hindsgaul, J. Org. Chem. 70 (2005) 9809–9813.
[33] R.R. Schmidt, J. Michel, Angew. Chem. 92 (1980) 763–764; Angew. Chem. Int., Ed. 19 (1980) 731–732.
[34] H. LeVine 3rd, Methods Enzymol. 309 (1999) 274–284.
[35] P. Westermark, C. Wernstedt, E. Wilander, D.W. Hayden, T.D. O'Brien, K.H. Johnson, Proc. Natl. Acad. Sci. U.S.A. 84 (1987) 3881–3885.
[36] L. Khemtémourian, G. Lahoz Casarramona, D.P. Suylen, T.M. Hackeng, J.D. Meeldijk, B. de Kruijff, J.W. Höppener, J.A. Killian, Biochemistry 48 (2009) 10918–10925.
[37] N.L. Fawzi, J. Ying, D.A. Torchia, G.M. Clore, J. Am. Chem. Soc. 132 (2010) 9948–9951.
[38] B. Meyer, T. Peters, Angew. Chem., Int. Ed. 42 (2003) 864–890.
[39] S.K. Chaudhary, O. Hernandez, Tetrahedron Lett. 20 (1979) 95–98.